To the Graduate Council:

I am submitting herewith a thesis written by Paul D. Driscoll entitled "Pressure Effects in Polymer Melt Rheology." I have examined the final copy of this thesis for form and content and recommend that it be accepted in partial fulfillment of the requirements for the degree of Master of Science, with a major in Polymer Engineering.

Donald C. Bogue, Major Professor

We have read this thesis
and recommend its acceptance:

John F. Fellers

Accepted for the Council:

Vice Provost
and Dean of The Graduate School

STATEMENT OF PERMISSION TO USE

In presenting this thesis in partial fulfillment of the requirements for a Master's degree at The University of Tennessee, Knoxville, I agree that the Library shall make it available to borrowers under rules of the Library. Brief quotations from this thesis are allowable without special permission, provided that accurate acknowlegment of the source is made.

Permission for extensive quotation from or reproduction of this thesis may be granted by my major professor, or in his absence, by the Head of Interlibrary Services when, in the opinion of either, the proposed use of the material is for scholarly purposes. Any copying or use of the material in this thesis for financial gain shall not be allowed without my written permission.

Signature Paul D. Arnold

Date October 15, 1986

PRESSURE EFFECTS IN POLYMER MELT RHEOLOGY

A Thesis

Presented for the

Master of Science

Degree

The University of Tennessee, Knoxville

Paul D. Driscoll

December 1986

ACKNOWLEDGMENTS

The author wishes to express his great appreciation to Dr. D. C. Bogue, his advisor, for encouragement, guidance, and many hours of patient advice, throughout this project. Appreciation is also extended to Dr. J. E. Spruiell and Dr. J. F. Fellers for their useful advice and comments, and to Dr. L. A. Utracki of the National Research Council of Canada for supplying his computer program for solving the Simha-Somcynsky equation of state.

The author is indebted to his fellow graduate students, particularly James Hackney, David Canter, Kenneth Zieminski, Y. D. Lee, and Larry Effler for invaluable help with the computer work involved with this project. The author would also like to thank Mr. Howell Thompson, and his coworkers Doug Fielden and Jack French in the Mechanical Shop, and Mr. Ted Long and his coworkers, Ron Johnson and Steve Steiner, in the Electronics Shop.

The author is also indebted to the Polymer Consortium and the Plastics Institute of America for financial support during this project.

Finally, the author would like to thank his family for their patience and support.

ABSTRACT

Wide ranges of pressure and temperature are encountered in many polymer processing operations. In addition, the pressures and temperatures often change rapidly with time, as, for example, in injection molding. While varying thermal histories have been explored in some detail, little work has been done on the corresponding pressure problem. The data which do exist for high pressures often show a dramatic increase in viscosity but the magnitude of the increase varies greatly, depending on the type of experiment and the experimental conditions.

The present work is largely concerned with the measurement and analysis of the viscosity of an amorphous polymer (polystyrene) in its melt state under high pressures. The measurements were made in a standard capillary rheometer plus a specially constructed downstream chamber, with the downstream chamber being held at a high pressure by forcing the material through a needle valve constriction. The data were analyzed in a general framework that includes not only high shear rate data from the present work, but also low shear rate data from the literature. A modified form of the so-called Bogue-White model was used to predict viscosity over all shear rate ranges. The model makes use of an important fact from rheological theory: viscosity can be expressed as the product of elastic moduli and time constants (in the present case, by one modulus and one time constant).

The pressure (and temperature) dependence of the time constant was motivated by the Simha-Somcynsky equation of state, which contains an explicit parameter related to the free volume. Utracki first noted

the usefulness of this theory for correlating the viscosities of both low molecular weight liquids and polymers. Although the Simha-Somcynsky equation is useful conceptually because it provides a free volume prediction for each pressure and temperature combination, it is concluded in the present work that several empirical adjustments are needed to use it quantitatively.

The experimental results at high pressure and high shear rates show substantial viscosity increases, although not nearly so high as expected from zero shear data. However, these two asymptotes can be understood within the framework of the rheological model used: at low shear rates, the magnitude of both the modulus and the time are important factors in determining viscosity, whereas at high shear rates, the modulus becomes the dominating factor.

TABLE OF CONTENTS

LIST OF FIGURES

CHAPTER 1

INTRODUCTION

As many kinds of polymer processing operations are considered, wide ranges of temperatures and pressures must be dealt with. Moreover the temperatures and pressures often change during the processing steps--i.e., the systems are non-isothermal and non-isobaric. In injection molding, for example, plunger pressures of 100 MPa (≈15,000 psi, ≈1000 atms) are not uncommon, with some specialty injection molding presses using pressures of over 700 MPa (≈100,000 psi). These high pressures are rapidly reduced to atmospheric as the mold is filled and released. While rapidly changing thermal histories have been widely studied, little has been done on the corresponding pressure problem. Experimental results that do exist show drastic increases in viscosity at lower shear rates, while less severe, but still significant viscosity increases have been found at higher shear rates (with the results varying in this range by up to a factor of ten).

Changes of pressure affect the rheological properties of the melt, the onset of the glass transition, and the character of the crystallization process, if crystallization occurs. Because of the many complex processes involved, attention here will be focussed specifically on melts, meaning, in the present context, amorphous polymers above their glass transition temperatures or crystalline polymers above their crystalline melting points.

Considering melts in this general sense there is an analogy between the effects of pressure and temperature changes: namely, decreasing the temperature is equivalent to increasing the pressure, and vice versa. In the simplest cases a variation in temperature or pressure leads to a change in the equilibrium volume, these changes being described by an equilibrium P-V-T relation. Such a relation is, in turn, connected to the so-called "free-volume" concept, the free volume being related to the difference between the actual specific volume of the melt and that which would exist if an equilibrium glass is imagined under the temperature and pressure conditions being considered. While the above characteristics concern equilibrium pressure effects, free volume has also been used to characterize the time dependence of various flow and elastic parameters. That is, the concept of free volume has been used to construct both pressure and temperature "shift factors" in time-dependent experiments, by extension of the familiar Williams-Landel-Ferry (WLF) equation.

But time parameters also enter the conceptual framework in another way: viscosity can be thought of as the product of moduli and time constants. Although several studies of the effect of pressure on viscosity exist, the experiments have not been analyzed in terms of these two different parameters. If these several viewpoints can be integrated, the effect of pressure on polymeric materials can be examined in a systematic manner.

CHAPTER 2

BACKGROUND

The Effect of Pressure on the Rheological Properties in the Melt

Numerous experiments on liquids have shown the increase of viscosity with pressure. In his classic work in 1931, Bridgman (1) reviewed many of the experiments of his contemporaries and predecessors. Bridgman pioneered many advances in high pressure physics including viscosity-pressure experiments for low molecular weight materials. Study of pressure effects on polymeric liquids began in the 1950's and 60's, with early experiments usually attributing the greater increases of viscosity with pressure, when compared to low molecular weight liquid, to the long chain nature of polymers. Along with the findings of viscosity increases with pressure, P-V-T experiments showed the shift of the glass transition of polymers with pressure.

The theory for pressure effects on polymer melt rheology has developed somewhat independently of the experimental results. Many of the theoretically based stress-strain (constitutive) equations developed to describe the viscoelastic behavior of melts are in principle able to deal with pressure effects, although because of the lack of data to which to fit them, they have not been used for this purpose. A major problem in dealing with pressure effects in constitutive formulations is determining the pressure dependence of the time constants. To supplement the limited experimental data which are available on this subject, one hopes to call on theoretical

analyses, most of which, finally, have to do with the concept of free volume.

Experimental Background

Pressure-Viscosity Experiments

Studies on the effect of pressure on polymer melt viscosity can be grouped into those which used capillary viscometers, those which used Couette rotational viscometers, and finally an experiment which used a pressurized falling sphere viscometer.

An early study on the effect of pressure on the melt viscosity of polystyrene by Maxwell and Jung (2), in which a modified capillary rheometer was used, showed that increasing the pressure from atmospheric (essentially 0.1 MPa) to 125 MPa (≈18,000 psi) at 195°C (385°F) increased melt viscosity 135-fold. A similar test which utilized polyethylene at 150°C (350°F) and 165 MPa (≈24,000 psi) showed a 14-fold increase in melt viscosity. It must be noted that these experiments did not seperate the effects of pressure and various shear rates. Nevertheless, these experiments established the greater sensitivity to pressure of chains containing bulky side groups compared to straight hydrocarbon chains. The first systematic study of pressure effects on polymer melt viscosity, undertaken by Westover (3), in which various pressure and shear regimes were studied, concentrated on polyethylene. In 1961 Carley (4) provided an important review article on pressure effects on viscosity, highlighting polymeric materials. Ito et al. (5) measured the effect of pressure on shear viscosity of an unspecified polystyrene with

typical processing shear rates. Choi (6), using the barrel and a capillary of an extrusion rheometer, like two capillaries in a series, found that the apparent viscosity of polyethylene at 190°C increased by approximately four times as the pressure in the barrel was raised from atmospheric to 165 MPa (≈24,000 psi) at a constant shear rate of about 7 sec^{-1}. Attempts have also been made to attribute the non-linearity in pressure drop vs. L/D plots in large pressure drop experiments to pressure effects in the tube, and to develop a pressure coefficient of viscosity. Experimenters using this method have included Penwell and Porter (7) and Penwell, Porter, and Middleman (8), with a review article on this subject provided by Goldblatt and Porter (9).

The second major type of instrument, a pressurized Couette (rotational) viscometer, was used by Cogswell and McGowan (10) to determine the effect of pressure on the viscosity of various liquids, including a number of polymer liquids. Data obtained for polystyrene, polymethylmethacrylate, HDPE, LDPE, polyoxymethylene, and polypropylene at several constant temperatures, and from atmospheric to at least 140 MPa (≈20,000 psi) were reportedly extrapolated to a zero shear viscosity. Between a 500-fold and a 55-fold increase in viscosity was observed for polystyrene; the former being the case at 170°C while the latter condition applied to 210°C. A later experiment by Cogswell (11), in which the same instrument was used, quantified the corresponding effect of a pressure rise or a temperature drop for several polymer melts. For instance, this study found that an in-

crease in pressure of 100 MPa (≈15,000 psi) was equivalent to a temperature drop of 53°C for a polyethylene melt.

The results of all these experiments, with 'commercial grade' polymers, are in question because the method of extrapolation to zero shear viscosity was not specified. Typically, commercial polymers are of wide molecular weight distribution, which show non-Newtonian (shear thinning) tendencies at atmoshperic pressure below shear rates of 0.1 sec^{-1} (somewhat temperature dependent) (see for instance, Graessley et al. (12)), the lowest shear rate evaluated under pressure in this experiment. Using a similar instrument Semjonow and co-workers (13) found a zero shear viscosity for polystyrene (M_w/M_n = 1.21) to be much more pressure sensitive than for several polyolefins. Interestingly, data presented in an earlier paper by Semjonow (14) for a polystyrene of unknown molecular weight, showed an increase in viscosity by a factor of only 2.2 at a constant shear rate of 40 sec^{-1} and 180°C as pressure was increased from 0.1 MPa to 100 MPa.

Finally, a falling sphere experiment under low pressure was carried out by Ramsteiner (15) at three temperatures, providing a limited amount of low shear rate data for polystyrene.

Shift of the Glass Transition with Pressure

Although the previous discussion has dealt with polymers well within their melt ranges, it is important to recognize that changes of state of matter such as the glass transition are shifted with pressure as well. For isothermal-nonisobaric experiments, the term glass transition pressure (P_g) is sometimes used (16). Havlcek et. al. (17) reported experimental work of Oels and Rehage (18) which showed a 90°C

increase in the apparent glass transition for polystyrene as pressure was increased to 400 MPa (≈60,000 psi) (See Figure 2.1). O'Reilly (19) and Goldblatt and Porter (9) reported a dT_g/dP factor determined with the data of various workers using several methods for a number of polymers. The same parameter was determined for polystyrene by Hellwege, Knappe, and Lehmann (20) as reported by Gee (21), and by Quach and Simha (22). The P-V-T data of Zoller (23) showed the shift of the glass transition with pressure for four amorphous polymers containing bisphenol-A residue in their repeat units. Additionally, Williams (24, 25), using polypropylene oxide and polymethyl acrylate, and Phillips and Dalal (26), using cis-polyisoprene, have studied glass transition shift with high pressure in dielectric experiments.

Theoretical Background

Constitutive Models

Because of the mathematical difficulties involved, the understanding of many polymer processing operations has remained at an empirical level. Empiricism has continued not only because varying thermal programs are being experienced during processing, but also because of varying pressure programs, examples being injection molding and extrusion. If we limit ourselves to only the region well above the glass transition temperature, a considerable literature on viscoelastic or constitutive (stress-strain) equations has developed over the years (for a review see Bird et. al. (27)). Integral formulations have been applied to many processes in simple geometries,

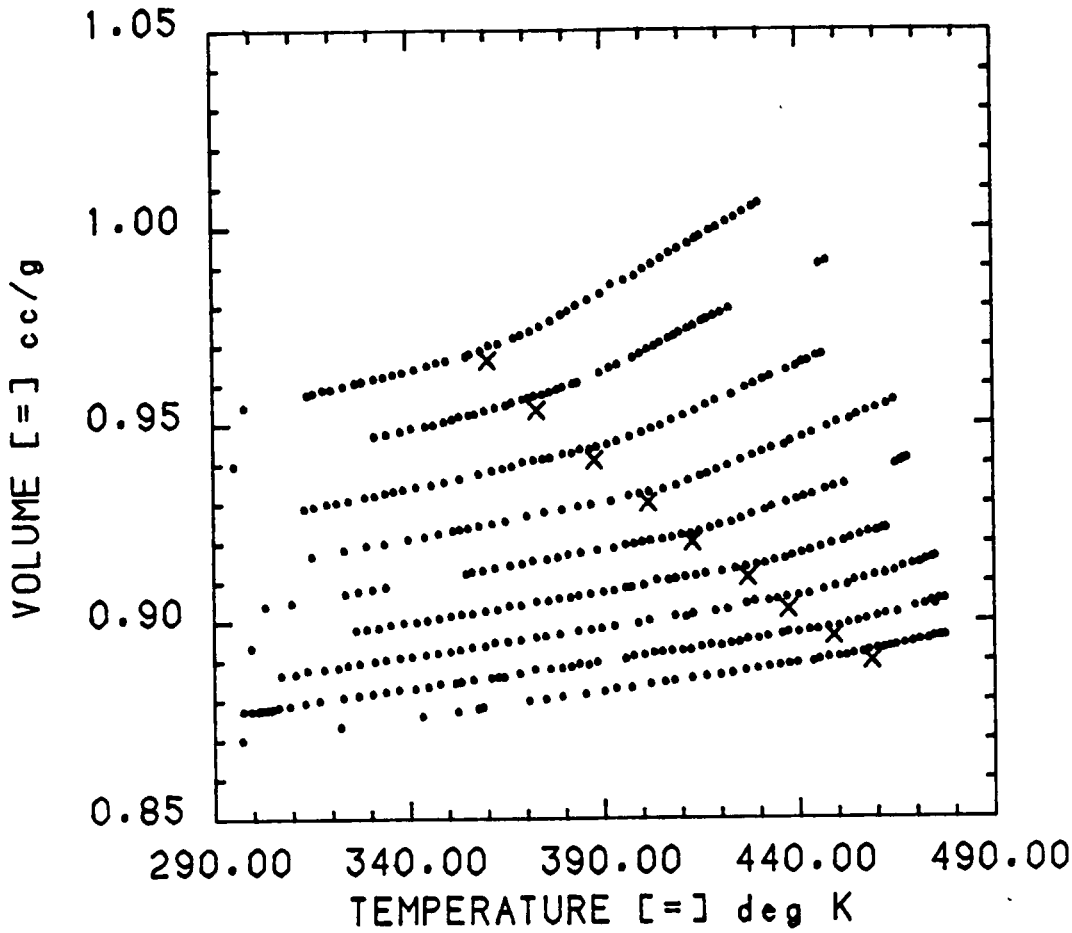

Figure 2.1 Typical volume-temperature data for polystryrene at various pressures. Adapted from Oels and Rehage (18). From top to bottom data groups represent isobars at 10, 50, 100, 150, 200, 250, 300, 350, and 400 MPa. "X"'s indicate location of interpolated glass transition.

as well as many materials (see Bird (27), Han et. al. (28), and Osaki et. al. (29)). Many of these equations are of the form

$$\sigma_{ij} = -p\delta_{ij} + \int_{-B}^{t} [m_1(t-t')C_{ij}^{-1} - m_2(t-t')C_{ij}]dt' \qquad (2\text{-}1)$$

Here σ_{ij} is the stress tensor, p is pressure, δ_{ij} is the Kronecker delta, m_1 and m_2 are memory functions, C_{ij}^{-1} and C_{ij} are the Finger and Cauchy strain tensors, respectively, and, t' and t denote an arbitrary past time and the present time, respectively.

In the simplest case, unsually known as the Lodge model (30), m_1 is finite but m_2=0. Using a series of Maxwell elements for the memory function m_1, one obtains

$$m_1 = \sum_n \frac{G_n}{\tau_n} \exp\left[-\left[\frac{t - t'}{\tau_n}\right]\right] \qquad (2\text{-}2)$$

where G_n are shear moduli and the τ_n are time constants.

Specifically, viscosity is related to viscoelastic theory as follows:

$$\eta = \sigma_{12} / \dot{\gamma} = \int_0^{\infty} \sum_n (G_n/\tau_n)\, e^{-s/\tau_n}\, (\dot{\gamma}\, s)ds = \sum_n G_n\, \tau_n \qquad (2\text{-}3)$$

where $\dot{\gamma}$ is the shear rate and s = t - t'. For a single G and τ this simplifies to

$$\eta = G(T,P)\, \tau(T,P) \qquad (2\text{-}4)$$

Shift Factors

Important variables in the constitutive models are the time constants which appear in the memory function (equation (2-2)). A general treatment for shifting involves writing

$$\tau = \tau_o \, a_T \, a_p \tag{2-5}$$

where a_T is the temperature shift factor, and a_p is the pressure shift factor. This equation simplifies for isothermal or isobaric experiments by setting the appropriate shift factors (a_T or a_p) equal to unity. Namely, if isobaric, a_p=1 and a_T varies; and if isothermal, a_T=1 and a_p varies.

The influence on time effects caused by the increase of pressure has been considered using a shift factor equation similiar to the temperature dependent Williams, Landel, and Ferry (WLF) equation (31) (see Chapter 4). In a similar manner Ferry and Stratton (32) have suggested a pressure shift factor equation

$$\log a_p = \frac{(B/2.303f_0)\,(P-P_0)}{f_0/k_f \; - (P-P_0)} \tag{2-6}$$

In this equation B is a constant often assumed to be unity, f_0 is the fractional free volume at the reference pressure P_0,and k_f is the isothermal compressibility of the free volume. Modifications of this equation are presented by Fillers and Tschoegl (33) and Havlicek et al. (17). Expressions of a simpler form,

$$\log a_p = C(P-P_0) \tag{2-7}$$

where C is a constant, have been developed by O'Reilly (19) and Bueche (34), and have been used with some success by O'Reilly on dielectric data of polyvinyl acetate.

Experimentally, a_p shift factors have been determined from viscosity data on polystyrene by Ito (5), on polyvinyl chloride from shear data of Zosel (35), and from stress relaxation data of Tschoegl and coworkers (33, 36-38) on several materials, particularly two lightly filled elastomers.

Pressure-Volume-Temperature Equations

In order to state a shift factor in a general way (when both T and P are changed), the WLF type equation needs to be considered in its most elemental form (39),

$$\log a_{12} = B/2.303\ (1/f_2 - 1/f_1) \qquad (2\text{-}8)$$

where B is a constant and f_1 and f_2 are the free volumes in the initial and final states. To determine the free volume, equations of state are needed which take into account the effect of both temperature and pressure on volume (i.e., P-V-T equations). The free volume, as stated previously, is defined as the difference between the observed specific volume and the specific volume occupied by an idealized equilibrium glass, or sometimes some fraction of the idealized equilibrium glass (the so-called occupied volume). The latter specific volume may be estimated from measurements of slowly-cooled, well-aged polymer glasses. A large part of the effort has gone into developing P-V-T relations for the former because an equilibrium state is readily obtained in the liquid.

An early attempt at a polymer liquid P-V-T equation was made by Spencer and Gilmore (40, 41). In an effort to develop a volume-pressure relationship for the injection molding of polystyrene they used a simplified form of the van der Waals equation of state. Good agreement was found with isothermal compressibility data of two polystyrenes for which the appropriate constants had been determined. The relation was later tested against compressibility data for polymethyl methacrylate, polyethylene, cellulose acetate-butyrate and ethyl cellulose and found to work equally as well. According to Carley (42) this equation is also applicable to equilibrium glassy polymers, although this claim is unsubstantiated.

Another well-known equation of state, the Tait equation (43), has been widely used since its applicability to polymer systems was recognized. Originally developed to describe the compressibility of seawater, this empirical equation has been used successfully on hydrocarbons of various molecular weights (44), including polymer melts and glasses (18, 21, 22, 45-46). It is of the following form

$$V(P,T) = V(0,T) \{ 1 - .0894 \ln[1 + P/B(T)]\} \qquad (2\text{-}9)$$

where V(0,T) represents the zero-pressure volume and B(T) is the Tait parameter, both functions of temperature. Unfortunately this equation, including evaluation of V(0,T) and B(T), requires determining four constants. Furthermore, in cases where the results do not fit experimental data, six constants are used to improve the fit (48). Fits for B(T) for polystyrene liquid and glass have been

determined by Quach and Simha (22). A new empirical generalization which reduces to the Tait equation has been presented by Cho (49).

In an ongoing effort to develop a theoretically based equation of state for polymers, Simha and coworkers (21, 45, 46, 50-53) have developed what has become known as the Simha-Somcynsky theory, from which most of Simha's present work stems. Based on a lattice model of Lennard-Jones and Devonshire (54), this cell theory has been modified to account for extra degrees of freedom of chain molecules, a requirement recognized by Prigogine et al. (55) (see Simha (56, 57) for details). In addition, extra entropy necessary to describe the melt has been added by the introduction of holes, giving finally a temperature and pressure dependent free volume fraction. The theory results ultimately in two complicated equations which must be solved simultaneously,

$$\bar{P}\bar{V}/\bar{T} = [1-2^{-1/6}y(y\bar{V})^{-1/3}]^{-1} + (2y/\bar{T})(y\bar{V})^{-2}\,[1.011(y\bar{V})^{-2}-1.2045] \qquad (2\text{-}10)$$

$$y^{-1}\ln(1-y) = (y6\bar{T})(y\bar{V})^{-2}\,[2.409 - 3.033(y\bar{V})^{-2}] + [2^{-1/6}y(y\bar{V})^{-1/3} - 1/3][1 - 2^{-1/6}y(y\bar{V})^{-1/3}]^{-1} \qquad (2\text{-}11)$$

Here y is the occupied hole fraction, and $\bar{P}$, $\bar{V}$, and $\bar{T}$ are reduced pressure, volume and temperature, respectively, namely, the ratio of the respective variable to a characteristic reference value (for example $\bar{P} = P / P^*$). For a tabulation of characteristic parameters see Utracki (58). In Figure 2.2 the theory is compared to several of the isobars from the experiment of Oels and Rehage (18) (see Figure 2.1, page 8), and also to data from Quach and Simha (22). (The

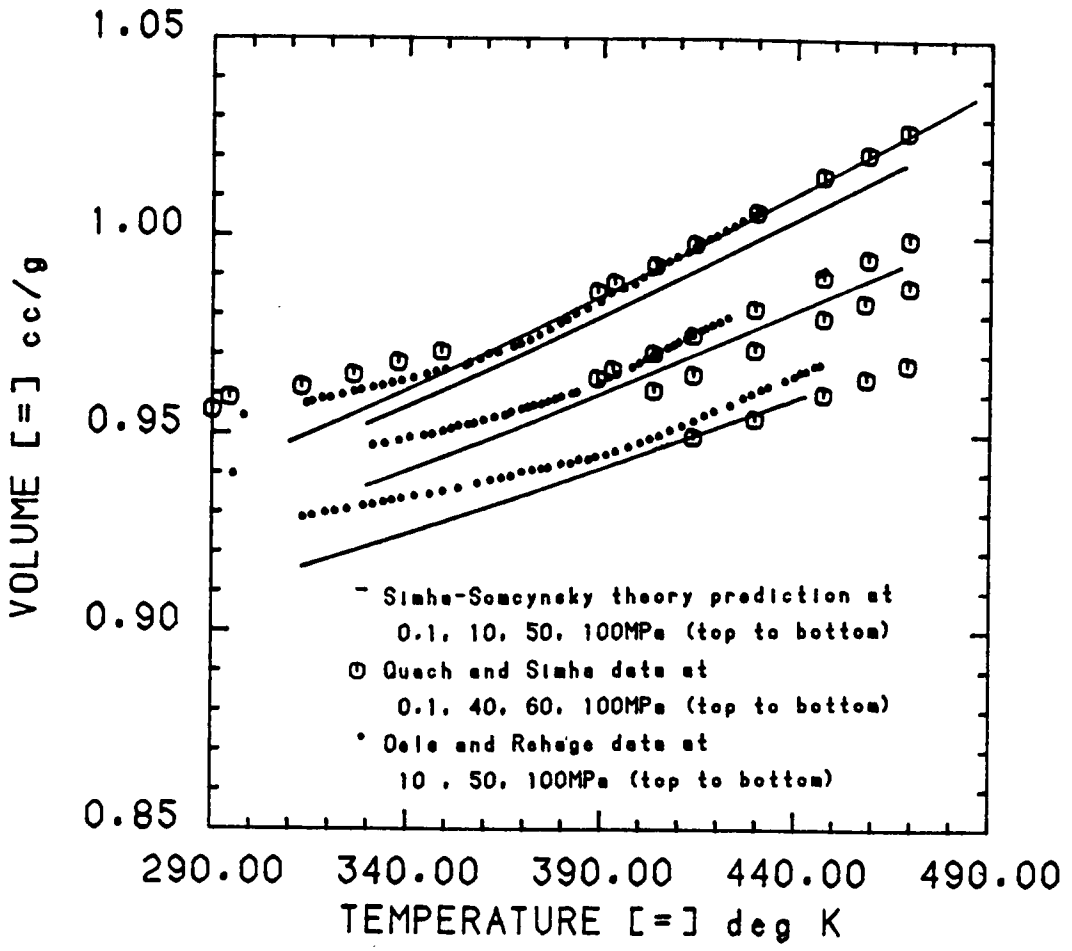

Figure 2.2 Fit of previous data to the Simha-Somcynsky Theory. The theory agrees well with the data of Quach and Simha (22) to which it was fit.

computer programs used to solve the Simha-Somcynsky equations simultaneously for the isobaric and isothermal cases are presented in Appendix A.) The disagreement with the Oels and Rehage data can be explained by the choice of reducing parameters, and possibly the low molecular weight of the experimental polystryrene (M_w = 20,400 and M_w/M_n = 1.06). When compared to the data of Quach and Simha, from which the reducing parameters were fit, agreement is good in the melt range. The theory is adequate in the melt but gives an incorrect shape for the glass. This inadequacy in the theory is discussed by McKinney and Simha (59) and by Zoller (60).

The S-S theory have been utilized by several other workers (61-64). Recently a simplification involving the linearization of the solution of the zero pressure isobar of this theory has been proposed (47, 61) to deal with polymer blends of polystyrene and poly (phenylene oxide). In these papers data for the asymptotes of pure polystyrene and poly (phenylene oxide), as well as the blends, have been compared to the simplification, and stand up favorably. A time-dependent form of the Simha-Somcynsky theory has been used to interpret aging of polymer glasses (65, 66). Finally the theory has been used to provide time constants for a constitutive equation for predicting yield in amorphous polymer solids (64).

Noting the similarity between the Tait equation and the zero-pressure isobar of the Simha-Somcynsky theory, namely the $T^{3/2}$ dependence, Hartmann and Haque (48) have proposed the following equation of state for polymer melts,

$$\tilde{P}\tilde{V}^5 = \tilde{T}^{3/2} - \ln \tilde{V} \qquad (2\text{-}12)$$

Like the Simha-Somcynsky theory this equation involves the use of reduced variables, $\tilde{P}$, $\tilde{V}$, and $\tilde{T}$. Data are presented for many polymer melts, demonstrating that the equation works quite accurately. Recently this theory has been extended to polymer solids (67).

Finally, the study of rate processes in polymer glasses has lead to several equations of state. P-V-T equations which include rate effects are presented by Bueche (34), and Chow (68-70). A modification of the Bueche theory has been proposed by Litt (71) to describe gaseous diffusion through polymers.

CHAPTER 3

EXPERIMENTAL

This chapter describes the experimental portion of the work. First, the physical characteristics of the material used to investigate the effects of high pressure on shear dependent polymer viscosity are summarized. Then, the high pressure attachment for the capillary Instron rheometer and the method of using it are described.

Experimental Material

The goal of this research was to measure the effect of high pressure on the viscosity of a typical commercial polymer over practical processing shear rates. For this purpose Shell TC3-30 polystyrene was chosen. This material is a commercial polymer of wide molecular weight distribution. The molecular weight properties of this polystyrene have been investigated by Takaki (72) and Racin (73), and were found to be M_w = 280,000 and M_w/M_n = 4.6. In addition, Bogue and coworkers (74-80) have extensively used TC3-30 to characterize its rheological properties under varying programs of time and temperature.

Equipment and Procedure

A modification of the standard Instron rheometer allowed the determination of shear dependent polymer viscosity to be investigated under high pressures. The complete apparatus consisted of a specially constructed high pressure attachment connected to a standard Instron capillary rheometer. The high pressure device introduced a second

capillary tube through which the melt was required to flow before entering the atmosphere. (See Figure 3.1.) This type of high pressure rheometer has been named a 'double die' type by Cogswell (81). The dimensions of the lower die were chosen such that, as the chamber region between the two die filled with polymer melt, a high pressure built up there. That pressure, measured by a pressure transducer located in the high pressure chamber portion of the apparatus, was transmitted back into the upper die becoming, then, the downstream pressure for the pressure drop determination. The pressure transducer was a Tuffage model made by Gentran, with a range of 0 - 140 MPa (0 - 15,000 psi). Viscosity under pressure for various shear rates can be calculated, in principle, in the same way it is for capillary viscometry with extrusion into the air (that is, by equations (2-3) and (2-4)).

The downstream chamber was kept under isothermal conditions by band heaters, controlled by a Variac. The Variac was adjusted according to the temperature registered on a digital temperature moniter connected to a thermocouple held in a port bored to within 1.6 mm (1/16 inch) of the interior of the pressurized chamber.

A critical part of the experiment was the sealing of the various portions of the apparatus in order to hold the pressure in the downstream chamber. This was a major problem in practice, and required the construction of several die holders and the use of several gasket materials. In the Instron barrel the plunger required complete circle polytetrafluroethylene 'O' ring packing (as opposed to the split ring seals often utilized in experiments in which extrusion

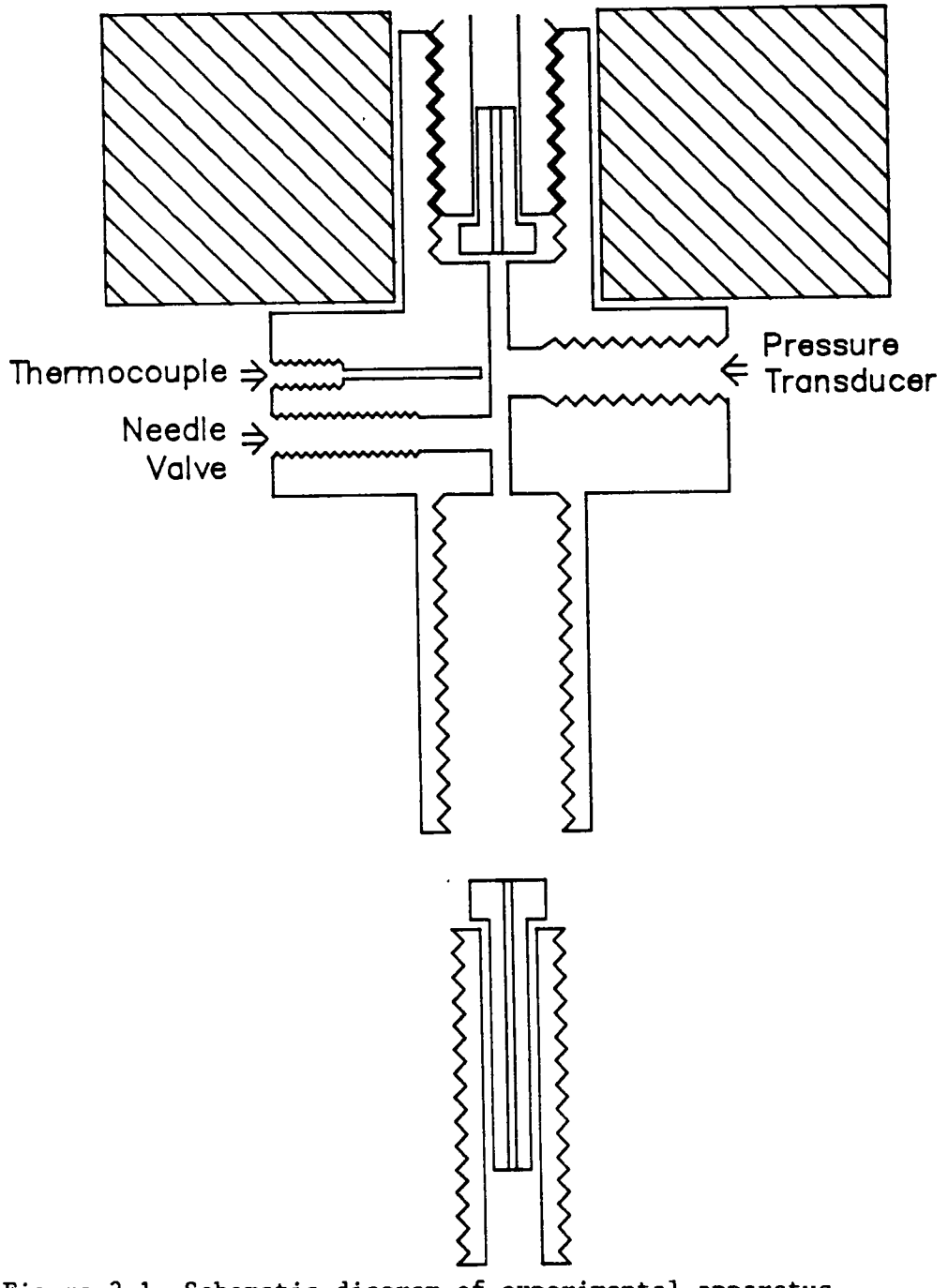

Figure 3.1 Schematic diagram of experimental apparatus.

is made directly into the atmosphere.) These same rings were also required in grooves near the top of the narrow end of the top die to prevent leakage before the polymer reached the high pressure chamber. It was also required to seal the top die with silver gaskets of approximately 3.2 mm (1/8 inch) height, placed in the undercut portion of the top and bottom of the wider section of the upper die. Although there were several pressure leaks caused by the yielding of the silver rings at the highest pressures achieved, pressures up to 125 MPa were usually obtainable. As a gasket sealing material, silver proved better than copper.

One of the initial drawbacks of the apparatus described above was the coupling of the downstream pressure with the flow rate; that is, the pressure drop through the downstream die varied with the flow rate (or the Instron plunger speed) and thus the absolute pressure in the chamber also varied with flow rate. A modification of the initial design was therefore made by adding a needle valve above the lower die to control the flow rate out of the chamber. This design change provided, with limited success, a method for selecting the downstream pressure independent of flow rate. In practice, however, very high pressures could not be maintained in the chamber unless the Instron plunger was being driven at least 0.00423 mm/sec (0.01 in/min), as well be discussed in more detail below.

An additional problem encountered with the use of the high pressure chamber was the creation of a flow resistance associated with the chamber, even though no pressure was being registered on the transducer. This resistance can possibly be attributed to a pressure

drop in the initial constriction in the chamber through which the polymer passed, or simply to an exit pressure drop in the die. The existence of the chamber resistance was noted by comparing successive runs at atmospheric pressure, one with the chamber in place and one with free flow into the atmosphere. The magnitude of this pressure drop was found to vary depending on the dimensions of the upstream die. A method of correcting for the measured pressure drops in the high pressure viscosity runs will be discussed in Chapter 5.

Actual pressurized runs involved the following procedure. After the entire chamber was completely assembled, isothermal conditions were achieved in the Instron barrel and the high pressure chamber. Polymer was allowed to melt in the Instron barrel, and then extruded, eventually traveling to the high pressure chamber. As the chamber filled the pressure began building, eventually reaching a steady state for a particular crosshead speed and a particular adjustment of the needle valve. After the addition of the needle valve it was hoped that as crosshead speeds were altered the pressures in the chamber could be chosen using only the needle valve, allowing the collection of isobaric data over the experimentally accessible shear rates. In fact, needle valve adjustment proved only partially successful. High pressures were increasingly difficult to achieve at the lower shear rates, because of the direct relationship between low pressure and lower viscosities. The obtaining of isobaric data also was hampered by the large pressure drops asssociated with the experiment, requiring an after-the-fact calculation of an average pressure (p_{ave}) which was designated as the "pressure" to be associated with that particular

run. The valve was, finally, used at several different settings at each crosshead speed to achieve data at several pressures. The results will be presented in Chapter 5.

CHAPTER 4

THEORETICAL DEVELOPMENT

In this chapter a framework for dealing with the effect of pressure on the viscosity of non-Newtonian polymer melts is presented. Use is made of Utracki's recent application of the Simha-Somcynsky theory which allows one to correlate high pressure zero shear viscosities. Coupling this with a suitable constitutive model, viscosity predictions are extended to the shear thinning regions by making the time constants a function of pressure as well as temperature. In addition the effect of pressure on shear modulus is considered and certain of Utracki's assumptions are reconsidered.

The Relationship of Free Volume to Shift Factors

Williams-Landel-Ferry (WLF) Equation

The goal of formulations such as the Williams-Landel-Ferry (WLF) equation has been the superposition of data taken at different temperatures and different times (time-temperature superposition). First stated explicitly by Leaderman (82), this idea allows the bringing together of experiments done at very different rates (or times) and temperatures. A further simplification, so-called "thermorheological simplicity", introduced by Schwarzl and Staverman (83), describes superpositions in which the time constants, regardless of number, are shifted by the same amount. Markowitz (84) has extensively reviewed the area of superposition. In addition to

horizontal shifts, changes of temperature (or time) dictate a vertical shift, namely, the shift of modulus. Tobolsky and Andrews (85) first dealt with the change in modulus using vulcanized rubber. This was later generalized to viscoelastic liquids by Ferry (39).

Summarizing, the horizontal shift of time constants τ can be stated by

$$\tau(T)/\tau_0 = a_T(T)/a_{T0} \tag{4-1}$$

The vertical shift of modulus is represented by the following relationship (87)

$$G(T)/G_0 = \rho T \; / \; \rho_0 T_0 \tag{4-2}$$

Here ρ is the density, and the subscripts refer to a reference state.

Motivated by a free volume theory, often associated with Doolittle (87), the shift factor $a_T(T)$ is usually correlated with the so-called Williams-Landel-Ferry (WLF) equation

$$\log a_T(T) = \frac{-C_1 \; (T - T_0)}{C_2 + T - T_0} \tag{4-3}$$

Here C_1 and C_2 are material constants and T_0 is a base state temperature.

Formulation from the Simha-Somcynsky Theory

While the success of the WLF equation in superimposing time-temperature data is well-documented, none of the pressure shift factor equations discussed in Chapter 2 has been widely used. Nevertheless the concept of a change in free volume with temperature or pressure is

certainly valid for polymers, as well as for other materials. One would feel intuitively, for example, that a decrease in temperature must somehow be related to an increase in pressure and vice versa. Although this line of thought led Cogswell (11) to form ratios of measured viscosities as a function of pressure and temperature, creating a kind of temperature-pressure equivalence, no explicit analytical expressions resulted. The idea of simple WLF-like expressions for pressure shift factors (39), while intuitively reasonable, has not led to generally useful formulations.

As a means of comparing pressure and temperature effects, the equation of state of Simha and Somcynsky (S-S) is especially useful in that it provides a free volume directly for polymer melts through the parameter y. Because of the original purpose of the S-S theory, (i.e., the fitting of P-V-T data for polymers) the role of the parameter y and certain conditions involving pressure and temperature were not initially utilized. Utracki (58) first noted the rheological significance of this expression. Originally interested in modeling the viscosity of low molecular weight liquids with changes in temperature and pressure, Utracki turned to the S-S theory when efforts to model pressure with traditional formulations, such as the Doolittle expression (87), failed. Because of the low molecular weight of the liquids involved, Utracki at first dealt with a more complicated form of the S-S theory than that presented in equation (2-11). In this formulation an additional parameter, a chain flexibility ratio, c, appears. For low molecular weight liquids Utracki was able

to linearize plots of log η vs. $1/(1-y)$ by adding a constant, δ to the denominator.

As molecular weight is increased into the high polymer range, the grouping $3c/s$ in the theory passes to unity (and equation (2-11) becomes valid). Therefore a natural extension of this work was to increase the molecular weight of the materials being studied. To avoid encountering non-Newtonian behavior, studies were limited to zero shear viscosity results. In addition Utracki found the δ assumption unsuitable for correlating most high polymer data, so he made what he called a "rheological assumption", $P_r^* = 2P^*$, which effectively decreases the pressure in the theory by a factor of two. With this empirical assumption, Utracki was again able to correlate high pressure data, in this case, zero shear viscosity data, in plots of log η^0 vs. $1/(1-y)$, for polystyrene (see Figure 4.1), polymethylmethacrylate, and high-density polyethylene (58). For a silicone oil and polypropylene, the assumption $P_r^* = P^*$ was suitable. In the case of polydimethylsiloxane, several polybutenes, and low-density polyethylene, either $P_r^* = P^*$ or $P_r^* = 2P^*$, was required, depending on the source of the data.

The above formulation assumes that the modulus G is constant for any combination of temperature and pressure, which is to say that superposition of zero shear viscosity data can be accomplished by shifting only the time constants. Actually, it is well-established (86) that G is a mild function of temperature (see equation (4-2) and accompanying discussion). Evidence for modulus as a function of pressure will be presented in Chapter 5.

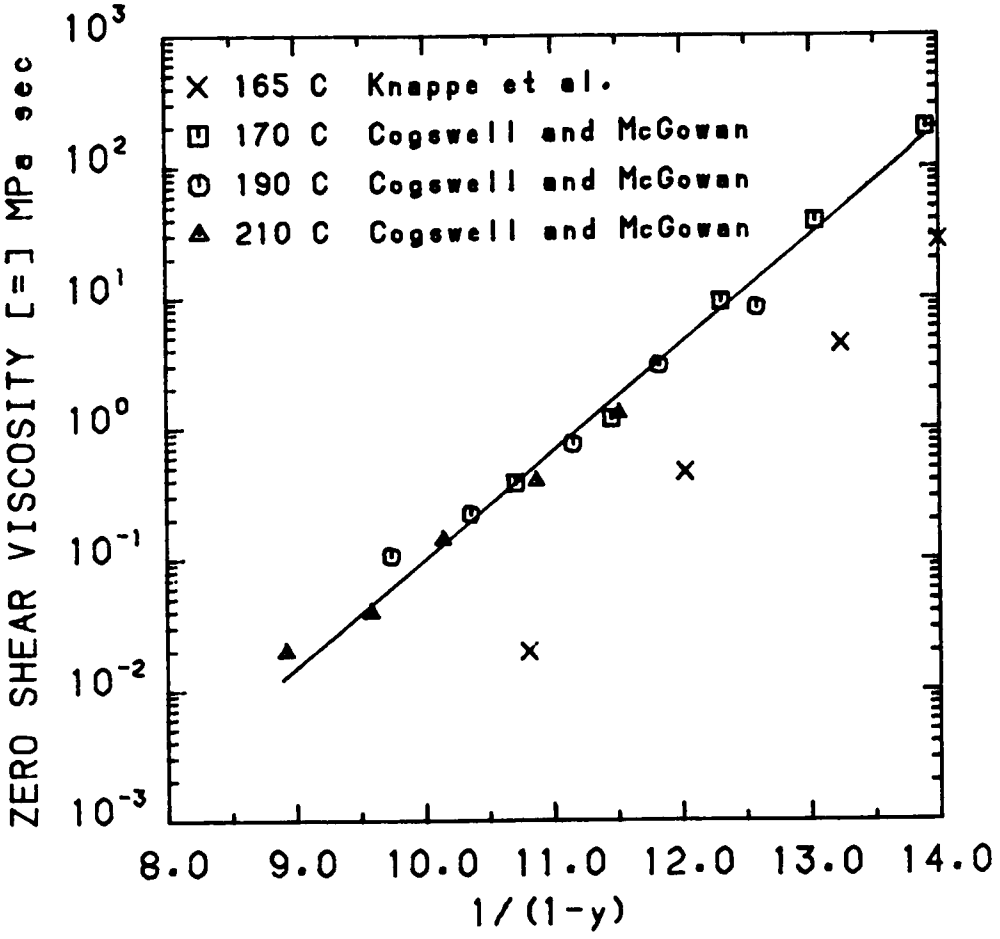

Figure 4.1 Zero shear viscosity as a function of free volume. Adapted from Utracki (58). Molecular weight characteristics of the polystyrenes are: Cogwell material, $M_w \approx 295{,}000$ (M_w/M_n unknown), and Knappe material, $M_w \approx 74{,}000$ and $M_w/M_n = 1.21$.

Simplification of the Simha-Somcynsky Theory

It has already been noted that by using an assumption regarding the effective P_r^*, high pressure zero shear viscosities for polymers become linear with 1/(1-y) (see Figure 4.1). These lines are of the form

$$\log \eta^0 = 1/(1-y) + C \tag{4-4}$$

where C is the y axis intercept. It is notable that data not only for different pressures, but also different temperatures all fall near the same line. After reviewing Utracki's low molecular weight findings, Tschogel (38) suggested that the difference of the inverse of free volume fraction from S-S theory could be recast in a shift factor form as follows:

$$\log \eta^0/\eta_0^0 = 1/(1-y) - 1/(1-y_0) \tag{4-5}$$

Here the superscripts refer to zero shear viscosity and the subscripts to a reference state. Borrowing notation from Utracki, the inverse of the free volume fraction may be expressed with the symbol Y

$$Y = 1/(1-y) \tag{4-6}$$

Utracki (88) has suggested that Y may be well-approximated by the form

$$Y = K_1(\overline{T}) + K_2(\overline{T})\overline{P} \tag{4-7}$$

where $\overline{T}$ and $\overline{P}$ are the reduced variables of the Simha-Somcynsky theory, which were discussed in Chapter 2. Plotting isotherms over

temperature ranges representative of polymer melts, it was found that the above curves were reasonably linear up to about 150 MPa. The intercepts of equation (4-7) were plotted with temperature, and $K_1(\bar{T})$ was found to be of the form

$$K_1(\bar{T}) = .1665 \; / \; (\bar{T} - .019145) \qquad (4\text{-}8)$$

In the case of $K_2(\bar{T})$, cross-plots with pressure show that the change of slope of the linear region of the isotherms produced by equation (4-7) can be described by

$$K_2(\bar{T}) = .44 \; / \; (\bar{T} - .0224) \qquad (4\text{-}9)$$

It should be noted that any rheological assumptions are still dealt with by adjusting the $\bar{P} = P/P_r^*$ factor. A direct comparison between the results of equation (4-7) and the result of the S-S theory will be presented in the following section.

The above work provides, then, a reasonable framework for simplifying the complicated Simha-Somcynsky theory as regards the prediction of the parameter y.

Reduction of Simha-Somcynsky Theory to the WLF Equation

It would be desirable to relate the S-S theory shift factor formulation presented in the last section to the familiar WLF equation. Carey, Wust, and Bogue (89) provide the framework for adjusting the WLF equation to a reference temperature of 160°C. The result, based directly on data for TC3-30, is

$$\log a_T = -6.3 \; (T - 160) / \; (T - 48.5) \qquad (4\text{-}10)$$

The basis for equation (4-10), like all WLF formulations, is the proportionality between a shift factor and the difference between the reciprocal free volume at an altered state of temperature and a base state (see equation (2-7)). To put equation (4-7) in the same mathematical form and physical framework, it is necessary to take the difference, $Y - Y_0$. The difference $Y - Y_0$ may be reasonably approximated by another equation, good at atmospheric pressure and in a range of temperatures well above the glass transition as follows:

$$Y - Y_0 = \log a_T = -11.54\ (T - 160) / (T + 39.2) \qquad (4\text{-}11)$$

This restatement is, then, of the WLF form. The various formulations are compared in Figure 4.2. At temperatures above about 100°C (nominal T_g), the range where one would ordinarily be using these shift factors, all three formulations--equation (4-7), equation (4-10), and equation (4-11)--are nearly identical.

In the limit at low temperatures, however, there are differences. Note that equation (4-10) goes to infinity at roughly 50°C, the so-called Vogel temperature, often associated with an ultimate T_g; this value is, however, considerably below the operational value for T_g, which for polystyrene is considered to be about 100°C. When put in the WLF form, the S-S theory produces a Vogel temperature of approximately -40°C (equation (4-11)). The physical meaning of this very low value is not understood.

The form of equation (4-7) also provides a convenient means of adding pressure effects to any of the shift factors discussed. At a constant temperature (in this case, 180°C) and a base state of

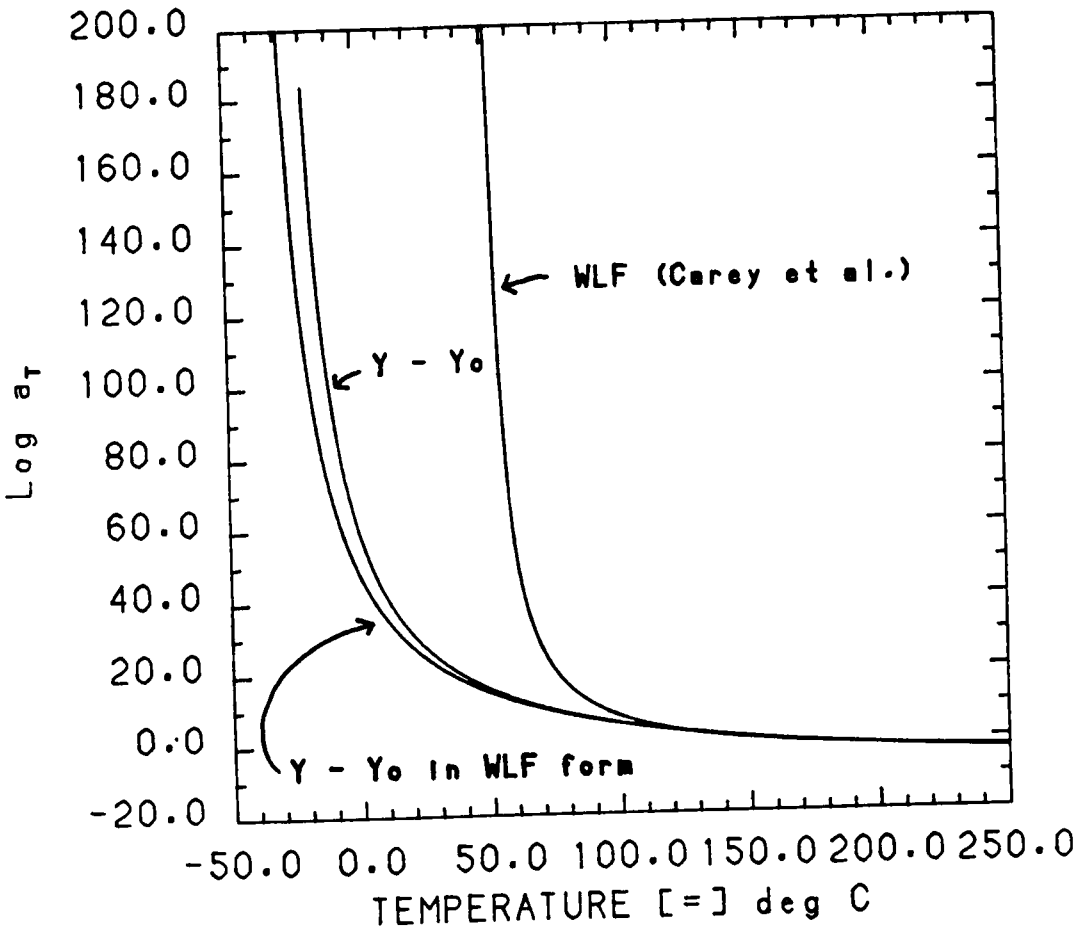

Figure 4.2 Shift factors as a function of temperature. The unusually large log a_T axis is used to illustrate the temperature at which the shift factor goes to infinity. The line marked WLF (Carey et al.) is the traditional WLF from (equation (4-10)). The $Y - Y_0$ form is equation (4-7) and is derived from the Simha-Somcynsky theory as presented by Utracki (58). The $Y - Y_0$ in WLF form is equation (4-11).

atmospheric pressure, Figure 4.3 shows that at any (constant) pressure, inclusion of pressure effects simply involves adding a constant value ($K_2(T)\bar{P}$), regardless of the temperature formulation. (Following Utracki, $P_r^* = 2P^*$ was assumed). In the case of equation (4-11), generalizing to include pressure effects from a base state of atmospheric pressure, one obtains

$$\log a_{T,P} = -11.54(T - 160)/(T + 39.2) + K_2(T)\, P/P^* \qquad (4\text{-}12)$$

A Simplified Constitutive Model for High Shear Rates

Development of the Model

As discussed previously equation (2-1) and equation (2-2) in steady simple shear reduce to

$$\sigma_{12} = \left(\sum_n G_n \tau_n\right)\dot{\gamma} = \eta\,\dot{\gamma} \qquad (4\text{-}13)$$

Comparing this to the constitutive equation presented in equation (2-1), no term involving isotropic pressure effects appears because, when $i = j$, δ_{ij} is zero. Many models for G_n and τ_n have been proposed (27, 28) differing in detail but not in general concept. A simple one is that due to Bogue and White (90) in which the G_n are considered to be independent of shear rate, and the τ_n are dependent on shear rate as follows

$$\tau_n = \tau_n^0 / (1 + a\,\tau_n^0\,\dot{\gamma}) \qquad (4\text{-}14)$$

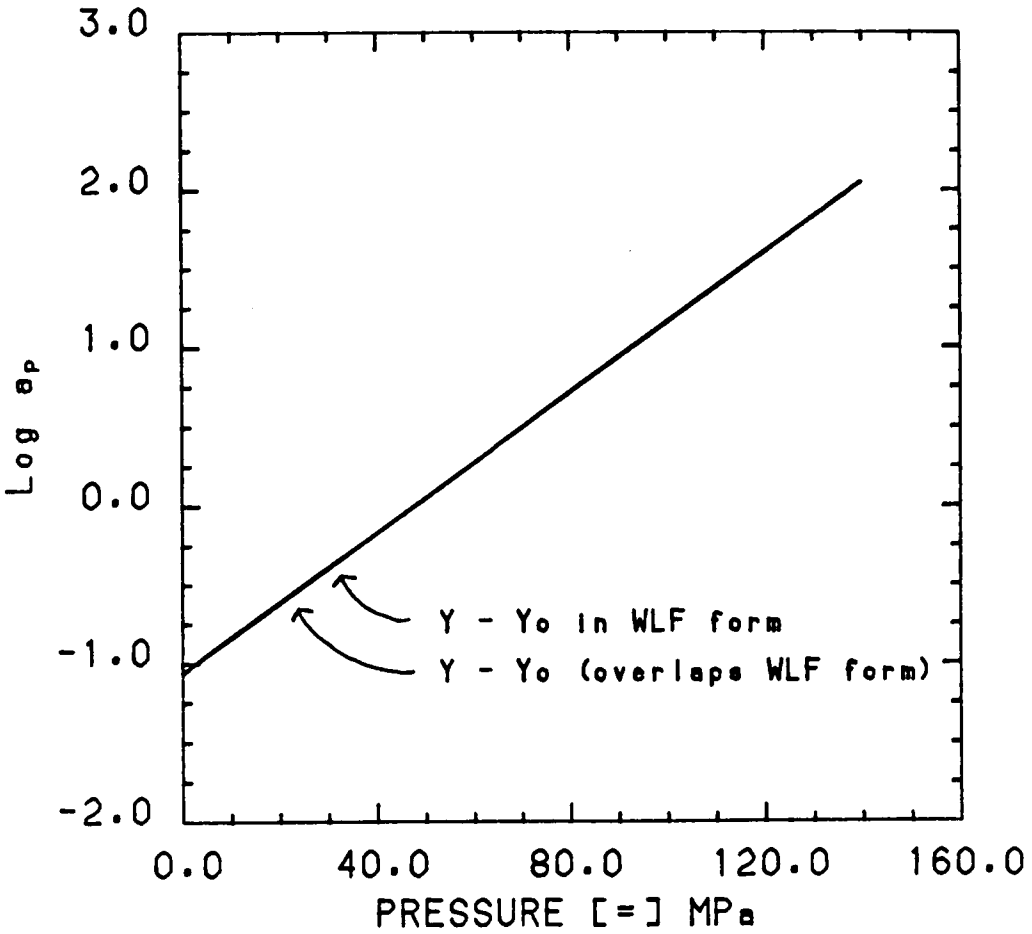

Figure 4.3 Shift factors as a function of pressure.

Here "a" is an adjustable constant and the superscript 0 refers to zero shear rate. A series of time constants is required to describe the relaxation in detail (often represented by a continuous spectrum, $H(\tau)$) because there are many modes of relaxation having to do with the behavior of small and large segments of the molecule and also having to do with the mixture of different molecular weights (the molecular weight distribution). For a complete discussion, see Ferry (39).

Nonetheless, one G and one τ are often used as a simplification in many applications (see, for example, Nam and Bogue (91)). A difficulty with the model is that at high shear rates, the slope of $\log \eta$ vs. $\log \dot{\gamma}$ curves is only roughly correct, equation (4-14) combined with equation (4-13) predicting that η should be proportional to $1/\tau$. In fact, there is a great deal of evidence that the asymptote is proportional to $1/\tau^b$, where b is less than unity. Dietz and Bogue (92) have studied applications of the model in which "a" is allowed to be a function of shear rate, which could include asymptotic slopes (b) less the one. Extensive data by Onogi and co-workers (93) on narrow molecular weight distribution polystyrenes suggest an exponent of about b = 0.82, close to the value predicted by Graessley (94). Using this value equation (4-14) becomes

$$\tau^0 = \tau^0 \; / \; \left[1 + a(\dot{\gamma}\tau^0)^{0.82}\right] \qquad (4\text{-}15)$$

where it is now understood that we are using only one G and one τ. Expressed in terms of viscosity this equation (henceforth refered to as the "modified Bogue-White model") becomes

$$\eta = G\tau^0 \; / \; \left[1 + a(\dot{\gamma}\tau^0)^{0.82}\right] \qquad (4\text{-}16)$$

The dependence of τ^0 on temperature and pressure, via shift factors, has already been discussed in Chapter 2. As noted previously, G, although often taken as constant, is dependent to some extent on temperature and pressure. A functional form for G(T,P) will be introduced later (see Chapter 5).

High Pressure Considerations Necessary to Apply the Model

For rheological studies involving tube flow, constitutive equations are often used to calculate the viscosity at various temperatures and, in the case of the present experiments, at various pressures. The standard analysis for tube flow involves solving the appropriate force balance equation to obtain the shear rate at the wall, an analysis due to Weissenberg, Mooney, and Rabinowitsch (WMR) (see, for instance, Tadmor and Gogos (95)). That analysis is a general one provided that the flow is developed - that is, that the profile is unchanging down the length of the tube, which implies that the rheological properties are constants throughout the flow field. The WMR analysis finally predicts the shear rate at the wall ($\dot{\gamma}_w$) as follows (95)

$$\dot{\gamma}_w = \frac{4Q}{\pi R^3}\left[\frac{3n' + 1}{4n'}\right] \qquad (4\text{-}17)$$

where Q is the volumetric flow rate, R is the radius of the tube, and $n' = d \log \sigma_w / d \log(4Q/\pi R^3)$. The accompanying shear stress at the wall , σ_w, is obtained from

$$\sigma_w = D \Delta p / 4L \qquad (4\text{-}18)$$

where D is the diameter of the tube, L is the length of the tube, and Δp is the pressure drop in the tube. Finally the viscosity function ($\eta(\dot{\gamma})$) can be determined by dividing equation (4-18) by equation (4-17).

If the flow is developed, it is therefore not necessary to use a particular rheological model, such as the power law model or the one shown in equation (4-16). However, if one considers variations of the viscosity function (due to temperature and pressure changes) down the length of the tube, then a particular model must be used. The result for power law flow in a tube is well-known (see Tadmor and Gogos (95)). The analogous problem for a fluid described by the Bogue-White model (equation (4-14)) has not heretofore been available. In the course of the present work, however, it was found that this problem could also be carried through to a closed solution, the analysis being shown in Appendix B. If one were to rigorously analyze data in terms of a particular model, then one would need to use the tube flow solution (that shown in Appendix B or an analogous result from another model) in an incremental (piecewise) fashion down the length of the tube. Such a detailed treatment was not felt necessary in the present work, however, as will be discussed below. Thus the results in Appendix B are shown for possible future reference only.

The modified Bogue-White model which best fits high shear rate data (involving the exponent 0.82 as in equation (4-16)) is non-linear in a complicated way and cannot be integrated across the radius of the tube, as was done in Appendix B for the original model. Fortunately, however, it is possible to show that the variation of properties along the tube is not so large as to make the WMR analysis invalid. The viscosity function depends, of course, on both temperature and pressure. As will be developed in the next section, the axial variation of temperature is not large, despite the large pressure drop (large viscous heat generation) involved, because there is significant heat transfer to the wall of the die. The effect of pressure is not so easily dealt with, however, because many of the runs involved singificant changes of pressure (up to ≈90 MPa) as shown in the tabular data of Appendix C. It is fortunate, however that the effect of pressure tends to be ameliorated at high shear rates, as can be seen by inspecting equation (4-16), which passes to the following result as the shear rate becomes large

$$\eta = (G/a)(\tau^{0.18}/\dot{\gamma}^{0.82}) \qquad (4\text{-}19)$$

As will be discussed in the next section, the effect of pressure on the modulus G is not large. The effect of pressure on the time constant τ is large, however, being exponential in character (see equation (4-12)), but because of the small exponent (0.18) in equation (4-19) above, the net effect of a large pressure drop is greatly lessened. A qualitatively similar result would come out of any rheological model with shear thinning because $\dot{\gamma}\tau$ come together as a

dimensionless quantity. The data treatment was therefore finally carried out using the WMR equation, assuming constant or average properties down the length of the tube.

Since isobaric data were difficult to obtain in the current experiments, the isobaric polystyrene data of Ito et al. (5) were used to estimate n' (see equation (4-17)), the slope of log shear stress at the wall vs. log apparent shear rate at the wall. For each isobar, n' was found to be fairly constant with changing shear rate, so the power law assumption was made (n'=n=constant). In these analyses the correction factor (3n + 1)/(4n) was found to vary from 1.46 at 0.1 MPa, to 1.73 at 100 MPa; at the higher pressure this value tends to the value 2.14 (using n=0.18). Isobaric (3n + 1)/(4n) values were plotted against pressure and correction value factors were interpolated as needed. These values were then used to adjust the experimental apparent shear rates to shear rates at the wall in the present experiment. The pressure was then taken as the arithmetic average of the pressure in the upstream and downstream chambers. In the case of temperature, however, no averaging was necessary because temperature was found to be essentially constant, being the temperature of the die wall (as shown below).

Heat Transfer Combined with Viscous Heat Generation

Because polymer melts are very viscous, one must consider the fact that significant temperature increases can be expected due to viscous heat generation. This effect is counterbalanced in many applications, however, because there is heat transfer to the wall of the flow channel. There is a rigorous mathematical treatment of the

classical problem of laminar heat transfer in a tube--adding, the complication of viscous heat generation--presented by Toor (96). The results, however, are numerical ones and can only be presented in graphical form, not in terms of simple analytical expression. Bogue (97) has shown that one can often approximate the results of the Toor analysis by simply adding the temperature rise one would expect from standard heat transfer theory. This kind of approximation is very useful for estimation purposes and will be used here to define an asymptote to the heat generation/heat transfer problem that may be encountered in many practical applications.

Adiabatic heat generation (flow in the absence of heat transfer) may be dealt with by a simple statement of the first law of thermodynamics. In the absence of external work, heat transfer, kinetic energy changes and potential energy changes, the first law (for incompressible fluids) reduces simply to

$$\Delta H = C_v \Delta T + (1/\rho)\Delta P = 0 \qquad (4\text{-}20)$$

where H is the ethalpy, C_v is the specific heat at constant volume, ρ is the density, ΔT is the temperature change, and ΔP is the pressure change. Equation (4-20) reduces to:

$$\Delta T = -\Delta P/(\rho C_v) \qquad (4\text{-}21)$$

In other words, the energy dissipated by the pressure drop shows itself as a temperature rise. Any small effect due to elastic effects is, of course, being neglected.

Now heat transfer in laminar tube flow, in the absence of heat generation, is a classical problem presented in almost all books on heat transfer (see, for example, Bird et. al. (98)). In traditional applications in chemical engineering one almost always considers an asymptote good at high Graetz numbers (the so-called Leveque solution). The Graetz number is defined by $N_{Gr} = WC_p/kL$, where W is the mass flow rate, C_p is the specific heat at constant pressure, k is the thermal conductivity, and L is the length of the tube. In traditional flows the Graetz numbers are high because the mass flow rates are high. For viscous polymers, however, the mass flow rates are, comparatively speaking, low. One is thus motivated to look at the asymptote for low Graetz numbers.

If the heat transfer coefficient is defined in terms of a log mean temperature difference, one uses the symbol h_{ln} and the asymptote for low Graetz numbers (and constant wall temperature) is (98)

$$h_{ln}D/k = 3.66 \tag{4-22}$$

where D is the tube diameter. This can be combined with a heat balance over the length of the tube and the nature of the temperature rise studied. Such a formulation cannot be done so easily, however, because the log mean temperature differences approach zero. Another way to proceed is to look at the low Graetz number asymptote for the heat transfer coefficient h_a defined in terms of an arithmetic average temperature difference. This asymptote is (99)

$$h_aD/k = (2/\pi)N_{Gr} \tag{4-23}$$

$$\text{or} \qquad h_a = \frac{2}{\pi} \frac{WC_p}{DL}$$

This asymptote holds almost precisely if $N_{Gr} < 3$ and is good enough for most practical calculations if $N_{Gr} < 10$.

Now the nature of equation (4-23) is by no means obvious; h_a does not depend--as does equation (4-22) and as one would suppose intuitively--on the thermal conductivity of the fluid (k), although k does enter indirectly through the Graetz number criterion. Rather one has the mass flow rate, among other variables, on the right-hand side. To understand the character of equation (4-23), let us consider a heat balance over the length of the tube:

$$WC_p(T_2 - T_1) = h_a (\Delta T)_a \pi DL \tag{4-24}$$

where T_1 and T_2 are the inlet and outlet temperatures and the arithmetic average $(\Delta T)_a$ is defined by

$$(\Delta T)_a = (1/2) [(T_w - T_1) + (T_w - T_2)] \tag{4-25}$$

where T_w is the wall temperaure, a constant. Combining equations (4-23), (4-24), and (4-25) one obtains

$$WC_p(T_2 - T_1) = (2WC_p/\pi DL)(1/2)[(T_w - T_1) + (T_w - T_2)] \pi DL \tag{4-26}$$

Simplifying one obtains the result that

$$T_2 = T_w \tag{4-27}$$

In other word the low Graetz number asymptote means physically that the heat transfer coefficient is sufficiently large that the outlet

fluid approaches the wall temperature. This result is independent of the value of the inlet temperature T_1.

Now in the case of the present work, one can estimate C_p = 0.44 cal/g°C and k = 3.1 x 10^{-4} cal/sec cm°C (100). Most of the work was done with a length L = 3.6 cm and the highest flow rates were in the range W = .01 to .03 g/sec in runs where there was a significant pressure drop and thus a significant temperature rise due to viscous heat generation (equation (4-21)). Using these values, the Graetz numbers ranged from 3.9 to 11.7. The first of these is within the low Graetz number range and the second is only slightly above ten (see the criterion following equation (4-23)). Thus there is significant heat transfer to the wall and even if the viscous heat generation is large (the maximum temperature rise calculated from equation (4-21) was about 30°C), one can, by thinking of it as an initially high temperature T_1, see that heat transfer will reduce the fluid temperature to substantially the wall temperature.

CHAPTER 5

DATA PRESENTATION AND ANALYSIS

The purpose of this chapter is to present the high pressure, high shear rate data obtained in the experimental part of this thesis. These results will be compared with theoretical predictions as well as to previous experimental findings. Viscosity data at atmospheric pressure and several temperatures are compared to theoretical predictions, based on the framework presented in the previous chapter. The effect of the pressurized downstream chamber will be examined, leading to corrections of the high pressure data to account for the flow resistance in this chamber. The final high pressure viscosity data will then be presented and compared to the theoretical predictions, the latter including both the theoretical effect of pressure on the time constant and the correlated effect of pressure on the modulus. Finally, previous treatments of the effect of pressure on zero shear rate viscosity will be reconsidered in light of the dependence of the modulus on pressure.

Presentation of High Shear Rate Data

Comparsion of Theory to Atmospheric Data

In this section atmospheric pressure predictions for viscosity - shear rate curves will be compared to data at 160°C and 180°C for a typical commercial polystyrene (Shell TC3-30). Comparisons between a multi-element fit (multiple G's and τ's) and a single element fit (one G and one τ) will be made.

In Figure 5.1 a curve representing the data of Takaki (72) for TC3-30 at 160°C is presented. Data over a wide range of shear rates were obtained by supplementing capillary viscometry data with data obtained by cone and plate rheometry. The data line is compared with a 25-element fit due to Takaki (72) and a single element fit carried out in the present work using the modified Bogue-White model (equation (4-14)). The parameters used in the single element fit were a = 1 and G = 0.05 MPa. The shear modulus used is a reasonable value compared with the plateau modulus obtained from the $H(\tau)$ spectrum for a polystyrene of wide molecular weight distribution presented by Onogi and co-workers (93). The value of τ (22.6 sec) was determined by a trial and error fit. Although the fit of the data with one G and one τ is relatively good in the high shear rate region, multi-elements are required to fit wide molecular weight distribution materials in the low shear regions, for the reasons discussed in Chapter 2.

Atmospheric data obtained for the present work at 180°C are compared with a single element fit of the modified Bogue-White model in Figure 5.2. The atmospheric data are presented along with a statistical fit (made by a SAS statistical computer program available as a Digital Electronic Corporation software package), which will be carried forward in the subsequent plots as a reference line. The parameters for the modified Bogue-White theory line are as follows: a=1 (the value used subsequently throughout this thesis); τ = 2.0 sec, obtained by the use of the WLF type fit of the S-S theory (equation (4-11)) to shift the time constant from 160°C to 180°C, and G = 0.05 MPa. The effect of temperature on modulus was neglected because, by

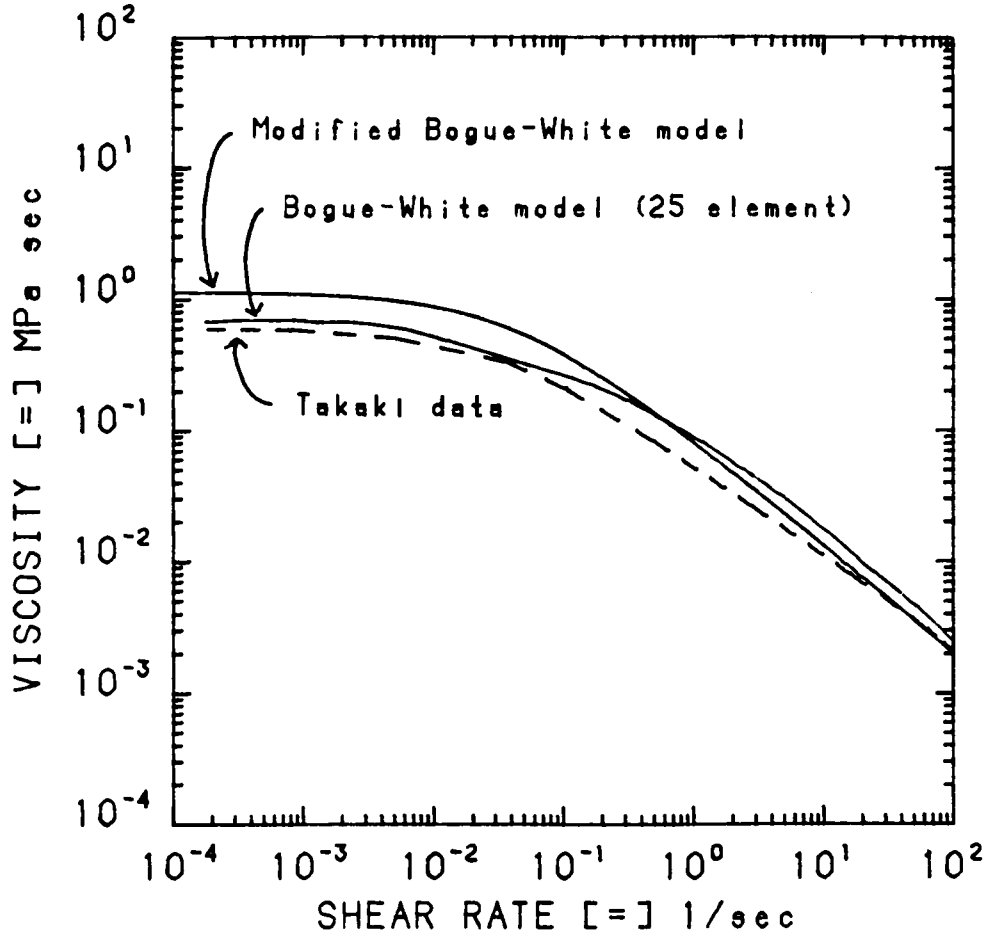

Figure 5.1 Shear dependent viscosity data and theoretical fit at 160°C and atmospheric pressure. The line marked "Bogue-White Model (25 element)" was taken from Takaki (72). The line marked "Modified Bogue-White Model" is equation (4-16) using τ=22.6 sec and G=0.05 MPa and a=1.

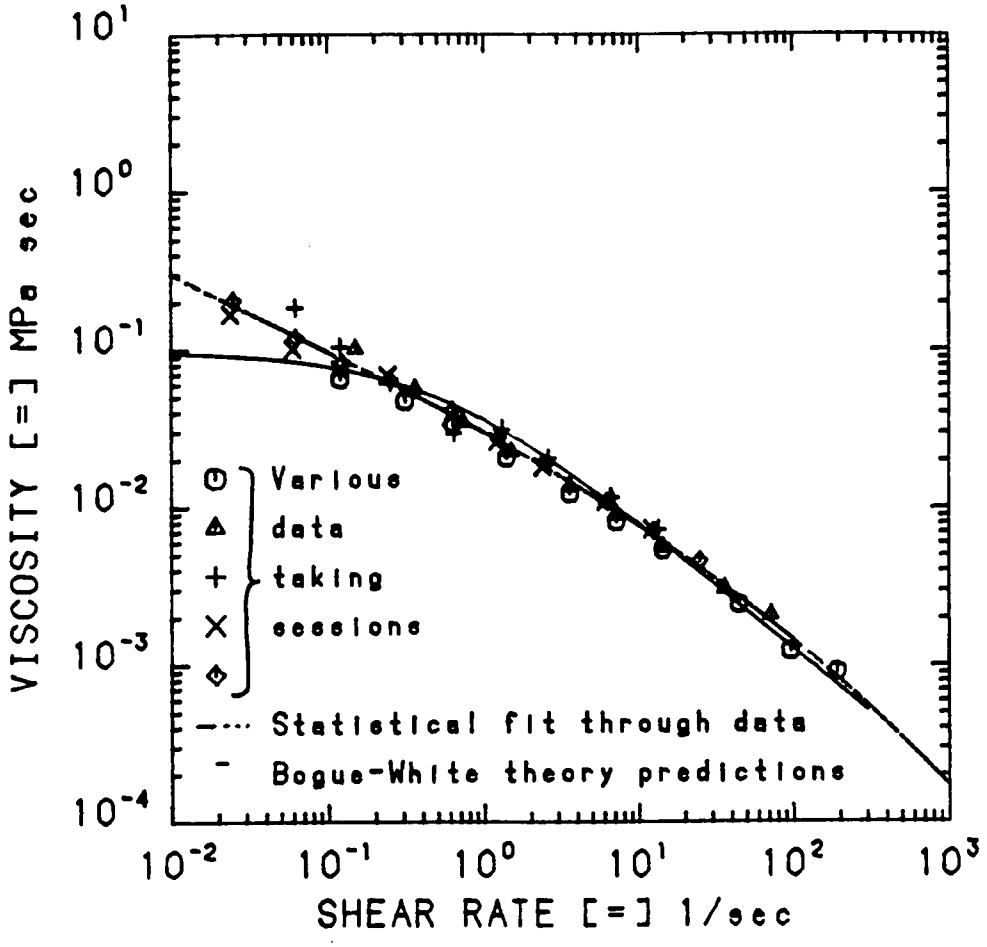

Figure 5.2 Shear dependent viscosity data and theoretical fit at 180°C and atmospheric pressure. Different symbols represent various data taking sessions.

means of equation (4-2), one can see that G changes less than 5% from 160°C to 180°C. A good, possibly fortuitous, fit is shown in the high shear region, whereas at lower shear rates, theory and data start to diverge. The disagreement at lower shear rates can probably be attributed to the use of a single element model.

Effect of High Pressure Chamber on the Data Analysis

The addition of the high pressure chamber described in Chapter 3 was found to increase the apparent viscosity at atmospheric pressure compared to that measured without the chamber under similar shear rates. The magnitude of this effect was found to differ depending on the dimensions of the upstream die.

Figure 5.3 shows the apparent viscosities for dies of different dimensions measured with, and without, the chamber. (All data were corrected to the wall shear rate by the analysis of WMR, as described in Chapter 4). At the appropriate shear rate, high pressure data to be presented were corrected by ratioing $\eta_{standard}$, the viscosity measured in the standard manner to $\eta_{chamber}$, to the viscosity measured with the chamber in place as follows

$$\Gamma = \eta_{standard} / \eta_{chamber} \qquad (5\text{-}1)$$

The measured high pressure viscosity was then multiplied by the correction factor Γ, yielding a corrected high pressure viscosity. In using this correction procedure one presumes that the change of the pressure drop in or near the chamber is proportional to the change of the pressure drop in the die itself. Since the latter is due to viscosity (and not elasticity), one is assuming the former is

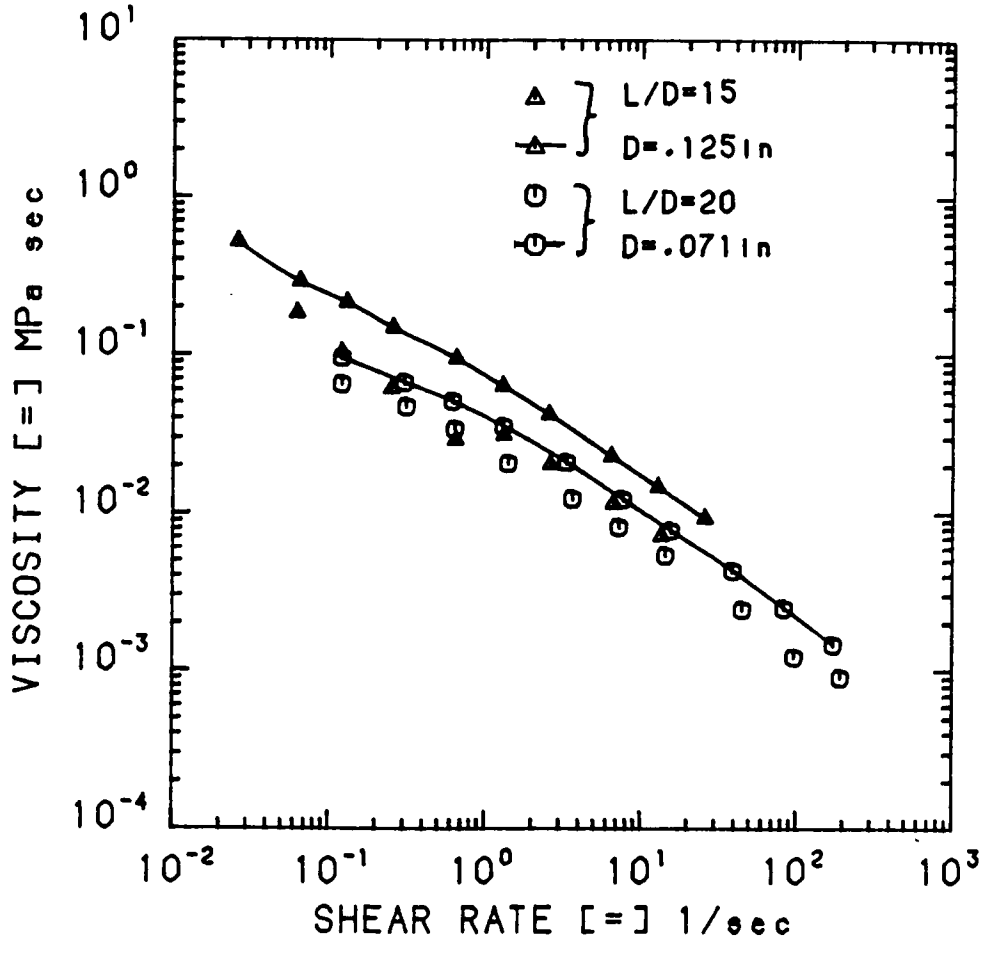

Figure 5.3 Comparison of viscosity data with and without the pressure chamber (180°C and atmospheric pressure). Symbols alone refer to atmospheric data with a particular die, whereas symbols with a line through them represent the high pressure unit in addition to that die.

similiarly dependent. This cannot be strictly true, but at high shear rates, elastic effects tend to become proportional to viscous effects and thus the correction scheme is probably reasonable. As can be seen from Figure 5.3, the die of greater diameter caused a higher chamber pressure drop, relatively speaking, than that of the smaller die; this is as one would expect since the pressure drop in the downstream chamber would be increasingly important as the pressure drop in the die itself becomes smaller.

Presentation of High Pressure Data

Data were taken at 170°C, 180°C, and 190°C and various pressures. At 190°C, the temperature used in the initial stages of experimentation, significant pressure buildup was difficult and substantial viscosity increases were not obtained. Although part of the pressurizing problem could be attributed to initial inexperience (improper tightening of the high pressure chamber, sealing problems, etc.), it became apparent that for the present experimental apparatus, high pressures and high viscosities were of a highly coupled nature: that is, one could not build up high pressures and high viscosities except at substantial shear rates. Noting that a significant increase in the zero shear viscosity occurs for a relatively small decrease in temperature (Cogswell and McGowan (10) and Hellwege et al. (13)), it was decided to decrease the experimental temperature from 190°C to 170°C.

Experiments at 170°C provided little retrievable information, however, because the pressure drop increased drastically and not always in a consistent manner. Using dT_g/dP factors already discussed

for polystyrene, a pressure drop of 125 MPa should raise the glass transition temperature by roughly 30°C. One would not suppose that this amount of increase in the glass transition would result in the drastic increase of pressure drop that was observed. The problem was not only one of a large increase of pressure, but of the pressure not reaching a steady state. Temporary plateaus in pressure would sometimes occur after several minutes, but would soon undergo an upward excursion to the limits of the transducer, and most likely beyond. This may be related to the qualitative observation of Maxwell and Jung (2) that their polystryene "acted like solid plug" above 20,000 psi (≈140 MPa) in their capillary experiment (not nearly a high enough pressure to induce the glass transition at their experimental temperature of ≈195°C).

From other previous experimental work, particularly that of Fox and Flory (101-102), Boyer (103) and Utracki (104) have noted a so-called liquid-liquid transition ($T_{\ell\ell}$) above nominal T_g, for polystyrene as well as for other liquids. It is tempting to try to relate this to the viscosity excursion. In the case of the volume-temperature curves presented by Utracki (104) to establish this transition, a careful inspection suggests two inflection points (one being T_g and the other $T_{\ell\ell}$); however, given the problem of rate dependence in such data, one would hesitate to reach a firm conclusion regarding the $T_{\ell\ell}$ transition. In addition, in his review article, Boyer (102) notes that the transition increases very significantly with molecular weight (from 162°C for a molecular weight of 4,900 (T_g = 62°C), to 169°C for a molecular weight of 32,000 (T_g = 94°C), to

192°C at a molecular weight of 360,000 Tg = 100°C)), also indicative of time effects. An easy explanation for the viscosity excursions in terms of T_g or $T_{\ell\ell}$ is therefore lacking.

Therefore, the majority of runs were carried out at 180°C, a temperature at which steady state force readings were reached and maintained at all but the highest crosshead speeds. In Figure 5.4 all of the corrected high pressure data obtained at 180°C are shown together on one plot for comparison with the line through the atmospheric data (the statistical fit to the atmospheric data carried forward from Figure 5.2 (page 46)). The high pressure data have been corrected for the presence of the chamber by the method described in the previous section.

For comparison to theory, the data were broken down into three groups corresponding to high, medium, and low pressure ranges (55-125 MPa, 35-54 MPa, and 0.1-34 MPa, respectively). These comparisons will now be made.

Modelling the High Shear Data, including Modulus as a Function of Pressure

The data are compared to the predictions provided by the modified Bogue-White model (equation (4-15)) in Figures 5.5, 5.6 and 5.7. The theory lines in these figures use the simplified fit to the Simha and Somcynsky prediction equation (4-12), a temperature and pressure dependent shift factor, shifted from a base state of T=160°C and P=0.1 MPa (1 atm). For reasons to be discussed in the next section, the assumption $P_r^*=3.25P^*$ was used instead of the Utracki assumption $P_r^*=2.0P^*$ (as in Figure 4.3, page 33). While the change of

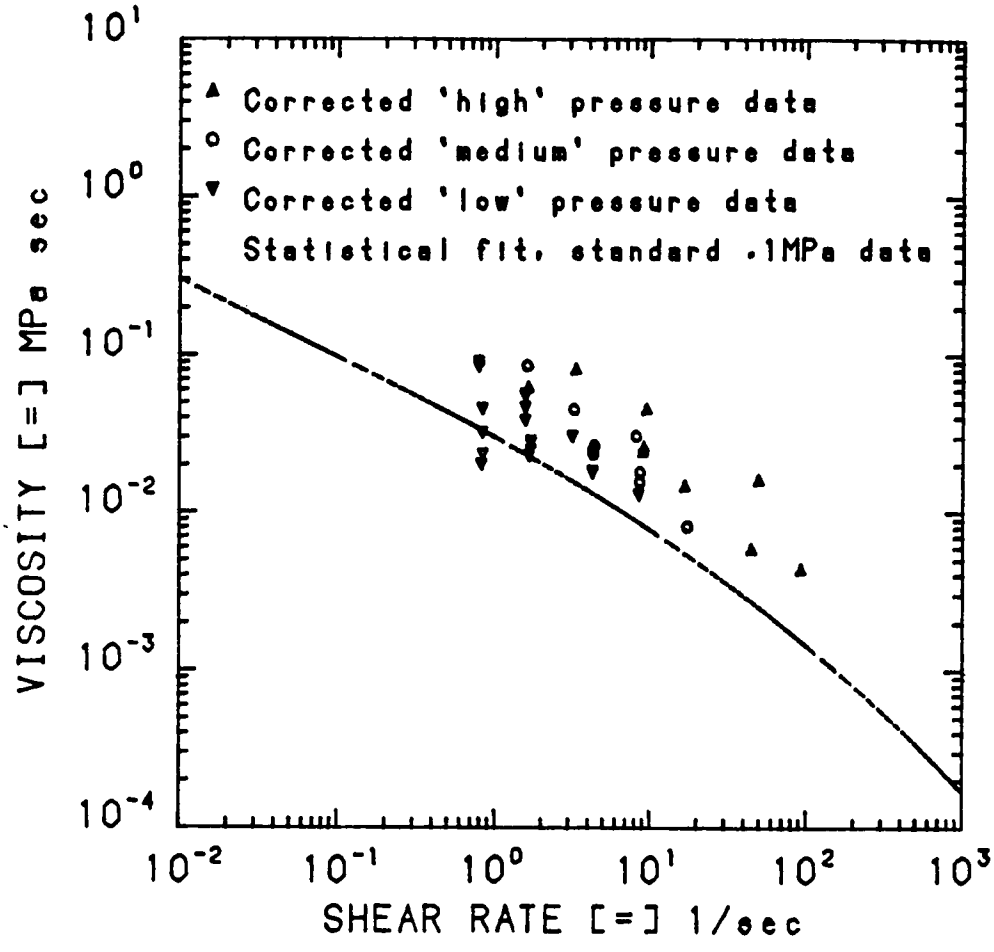

Figure 5.4 Summary of high pressure viscosity data at 180°C. All of corrected high pressure data presented along with a statisical fit of the atmospheric data.

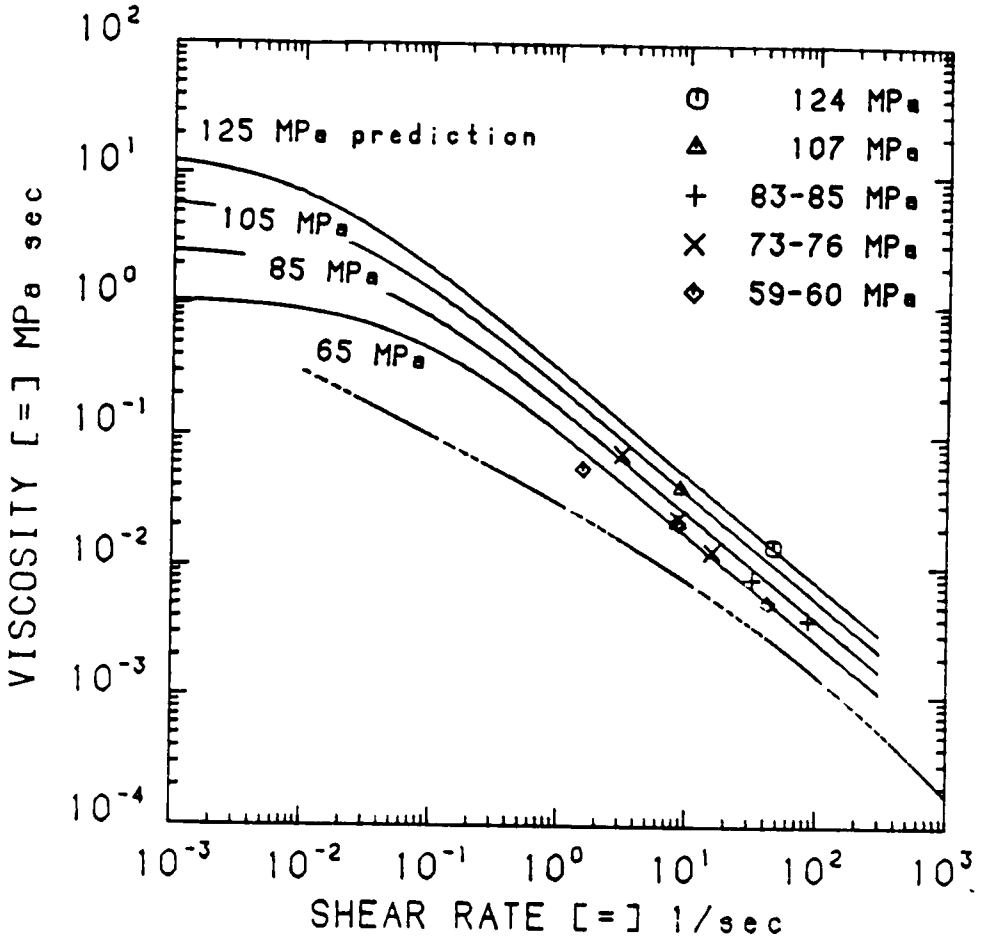

Figure 5.5 Comparison of high pressure viscosity with theoretical fit. The time constant is pressure dependent and the modulus is a function of pressure. The dotted line is a statistical fit of the atmospheric data.

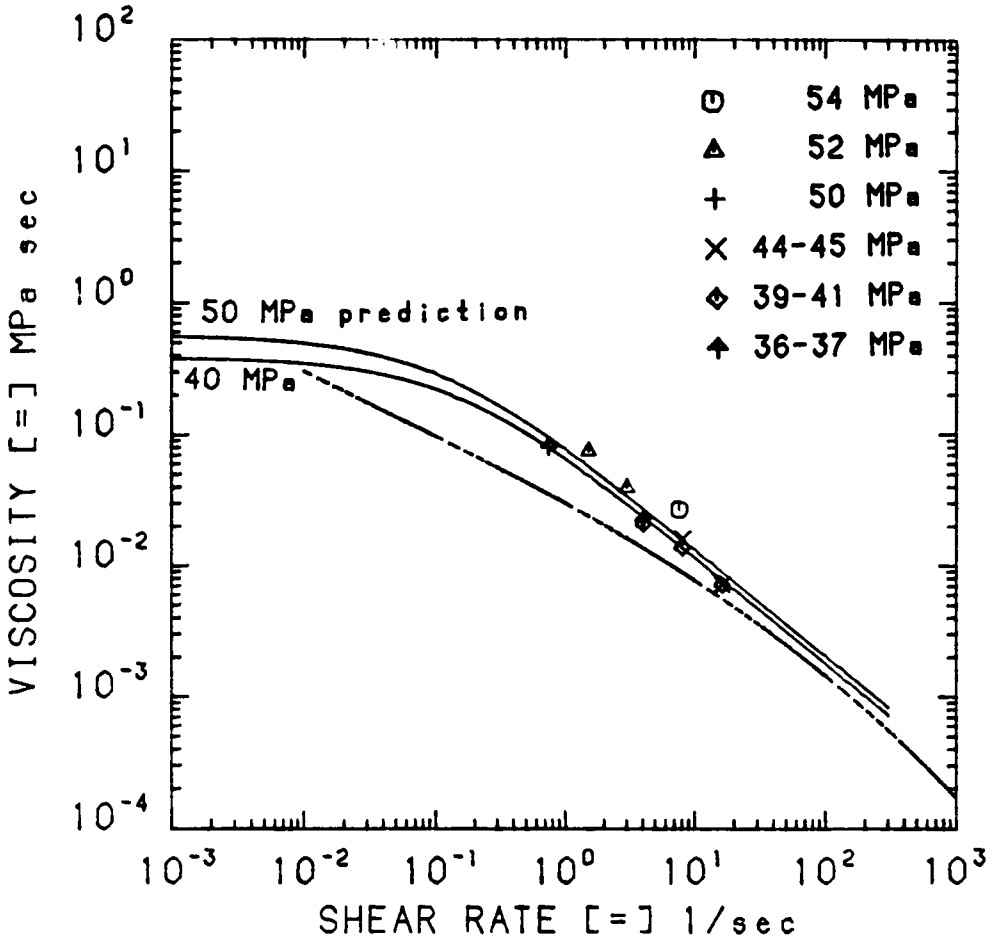

Figure 5.6 Comparison of medium pressure viscosity with theoretical fit. The dotted line is a statistical fit of the atmospheric data.

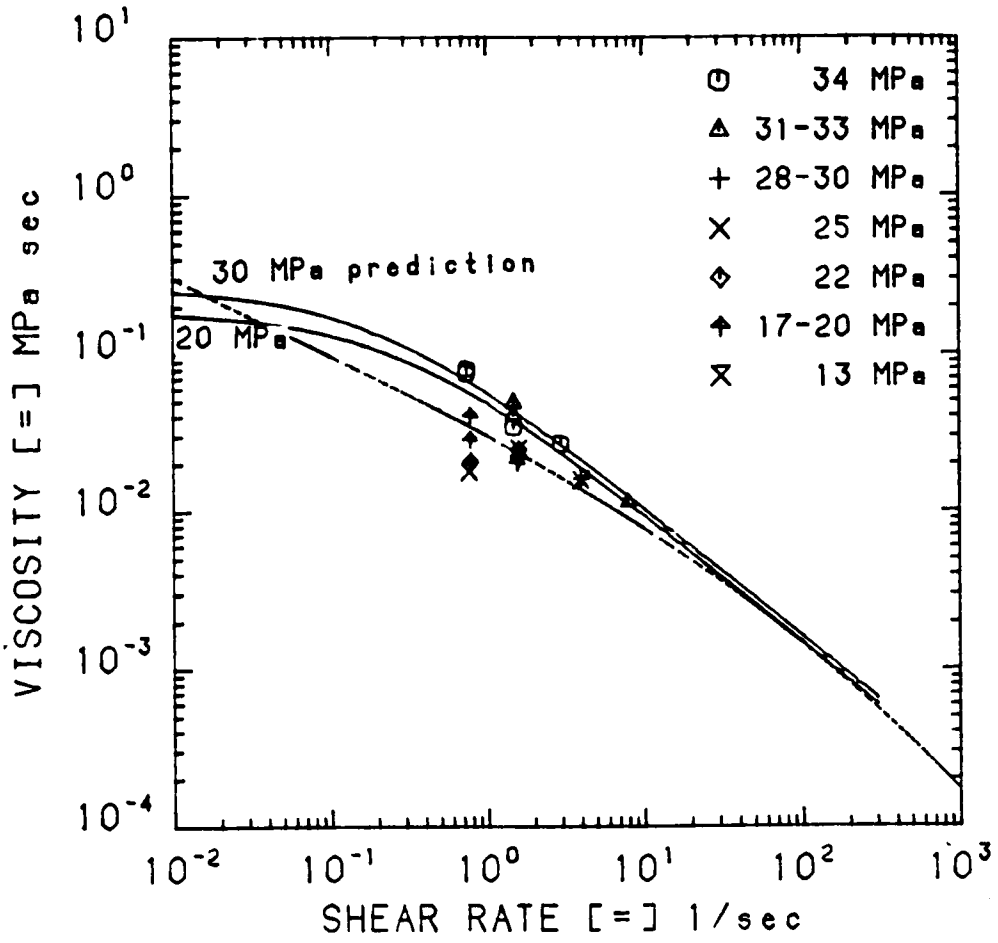

Figure 5.7 Comparison of low pressure viscosity with theoretical fit. The dotted line is a statistical fit of the atmospheric data.

modulus due to a 20°C change in temperature shift was deemed insignificant, the effect of pressure on modulus cannot be neglected if theory and data are to be brought together in satisfactory way.

The shift of modulus with temperature in the rubbery state has traditionally been dealt with by using either the factor T/T_0 or $T\rho/T_0\rho_0$, the former coming from rubber elasticity theory and the latter from modified Rouse theory (39). The effect of the density ratio is so small that it is not clear from the data whether it is necessary or not (39). Because there is an obvious connection between rubber elasticity theory and melts in the rubbery state, the simpler factor T/T_0 will be used here. Introducing a pressure factor, the form for a combined factor would be

$$G(T,P)/G_0 = (T/T_0)\ g(P) \qquad (5\text{-}2)$$

where g(P) is a function to be determined experimentally.

The increase of modulus with pressure seems intuitively plausible on the basis that the number of entanglement points per unit volume increases as the pressure and density increase. A similar argument, though one which moves the modulus in the opposite direction, could be invoked for temperature. The factor which actually appears (T/T_0), results from the increased mobility of the molecules as the temperature is increased, and not from a change of density. In a general way it should be noted that the effect of pressure on volume is highly non-linear, much more so than that effect of temperature on volume (see Figure 2.1, page 8).

Although data are limited, the pressure dependence of shear modulus has been measured by other experimenters (13, 35). Because the data are for several materials, Figure 5.8 presents the ratio of high pressure to atmospheric pressure shear modulus as a function of pressure. Thus the present correlation for G as a function of pressure is not unreasonable. A polynomial fit to the line in Figure 5.8 gave the following result at 180°C, with P being expressed in the units of MPa

$$G(P)/G_0 = g(P) = 1 - 2.37\text{x}10^{-3}P + 1.041\text{x}10^{-4}P^2 \qquad (5\text{-}3)$$

In other words, the theory lines in Figures 5.5, 5.6, and 5.7 were obtained by rewriting the one element form of equation (4-12) as follows:

$$\eta = \sigma_{12} / \dot{\gamma} = (G_0\ g(P)\ \tau_0\ a_{T,P}) \ / \ \left[1 + a\ (\dot{\gamma}\tau_0\ a_{T,P})^{0.82}\right] \qquad (5\text{-}4)$$

where the modulus shift factor g(P) is given by equation (5-3) and the time constant shift factor $a_{T,P}$ is given by equation (4-14). The reference state was taken to be 0.1 MPa and 160°C, at which conditions G_0 = 0.05 MPa and τ_0 = 22.6 sec apply.

Generally the fit of the model to the data is good. It is important to note that two die sizes were used at all except the highest pressure range (85-125 MPa) in which case only the smaller die was used. The generally good agreement between the two dies is good evidence that the neglect of entrance effects plus the correction procedure used for the downstream chamber were satisfactory

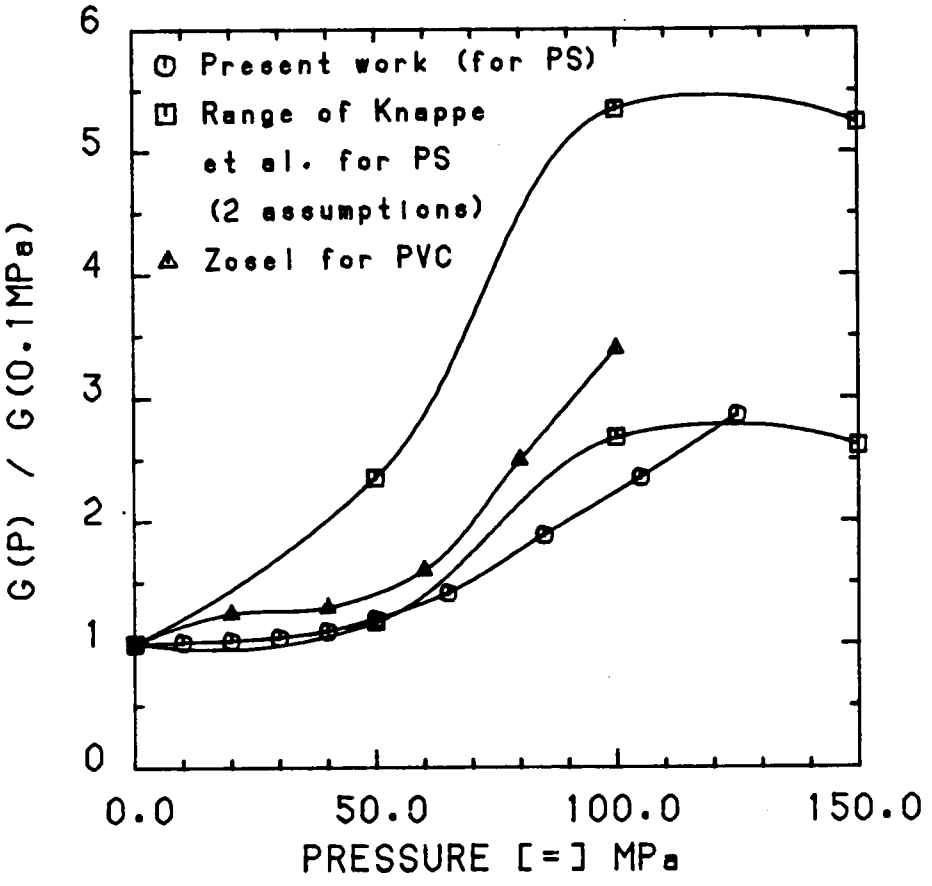

Figure 5.8 Shear modulus as a function of pressure. Two lines are shown for the Knappe data because the atmospheric modulus was specified as a range of values.

assumptions. In the highest pressure range (85-125 MPa) at shear rates between 10 and 50 sec^{-1} the ratio of the pressurized to the atmospheric viscosity is about 6, of which approximately a factor of 3 is provided by the g(P) function and a factor of 2 by the shift of the time constant. Other high pressure experimenters using polystyrene in this shear range are Ito et al. (5) and Semjonow (14). Ito et al. found between a 10 and 15-fold viscosity increase in polystyrene (depending on shear rate) at this temperature (180°C). On the other hand, Semjonow, also experimenting with polystyrene at this temperature, found a 2.2-fold increase at a shear rate of 40 sec^{-1}.

The only condition at which scatter was an important factor occurred at a shear rate of about 1 sec^{-1}. The corrected data, which are the data shown, are in some cases below even the atmospheric line. The cause of this difficulty is not known, although the data from the small diameter die would be in reasonable agreement with the model if left uncorrected. These data are at the limit of obtaining measureable forces in the Instron barrel and the scatter probably reflects the inherent inaccuracy in determining the pressure drops in this range of operation.

Analysis of Low Shear Data

In light of the decision to allow modulus to be a function of pressure, it is necessary to reexamine the formulation presented by Utracki (58) in which he plots the logarithm of zero shear viscosity results against the reciprocal of the free volume (Figure 4.1, page 27). In that analysis Utracki found it necessary to make the

assumption that the pressure is reduced by one half in order to correlate zero shear viscosity with the y parameter from the theory of Simha and Somcynsky. Making the modulus a function of pressure in the present formulation requires that the time constant be shifted differently with pressure; recall equation (2-4) in which viscosity is a product of the modulus and the time constant. If modulus is a function of pressure, then the "effective pressure" must be less than half the actual pressure, which was Utracki's assumption. It is one of the purposes of this section to quantify this pressure adjustment parameter, and to discuss its significance in the modified Bogue-White model (equation (4-16)), with and without modulus as a function of pressure.

Although there seems to be an adequate fit to the data by the S-S theory if one uses $P_r^*=2P^*$ (see Figure 4.1, page 27), closer scrutiny shows otherwise. When data in ratio form are compared to theory (Figure 5.9), there is a significant overestimation by the theory. In Figure 4.1 (page 27), atmospheric data tend to fall above the line, while the high pressure data tends to fall below the line, an effect which is masked by the large range of the logarithmic scale of the ordinate. Recasting the zero shear data as a ratio of the viscosity at a high pressure to that at at atmospheric pressure, with temperature as a parameter, gives the plot show in Figure 5.9. That figure emphasizes the differences between the theory (assuming $P_r^* = 2P^*$) and the data. In order to fit those data adequately, an assumption other than $P_r^* = 2P^*$ appears to be necessary.

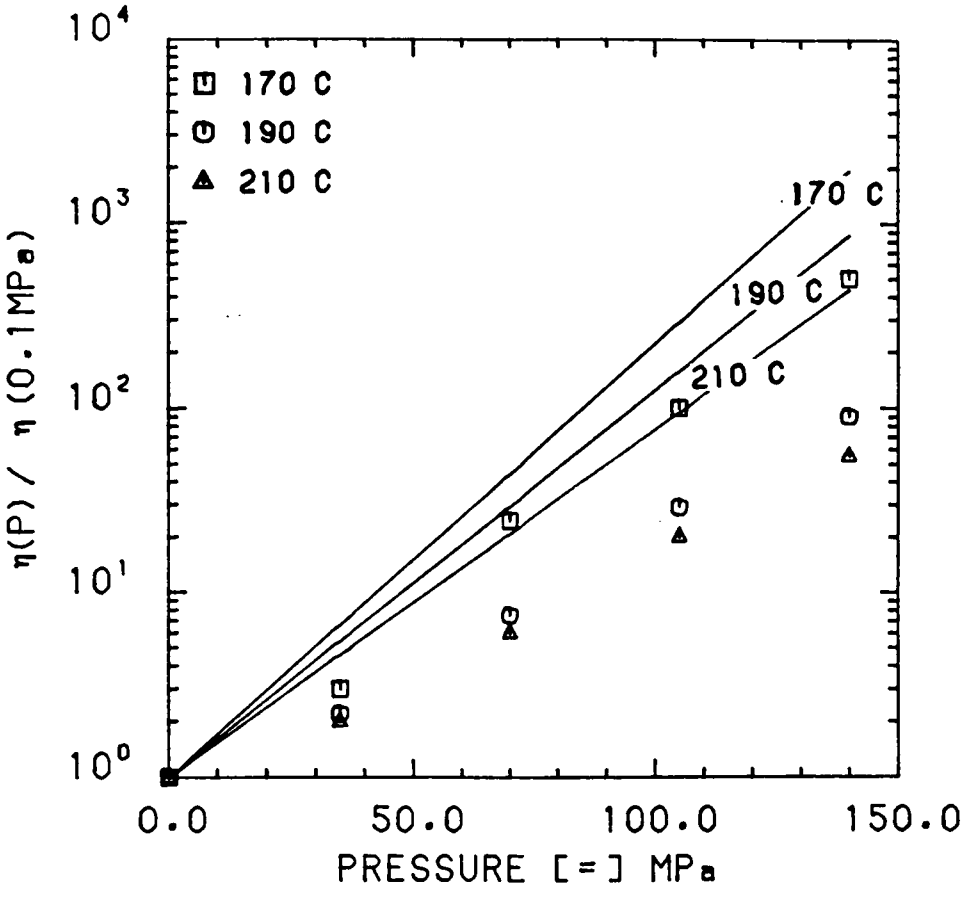

Figure 5.9 Ratio of zero shear viscosities vs. pressure, compared to constant shear modulus theory lines. Here, modulus is taken to be constant with pressure. Data from Cogswell and McGowan (10). Following Utracki (58) $P_r^* = 2P^*$.

A range of adjusted reducing pressures have been used to describe various transport phenomena in the literature. Superposition in high pressure stress relaxation experiments for several materials by Moonan and Tschogel (38) required P_s^*/P^* values from 1.29 to 2.24 (here P_s^* represents a stress relaxation reducing parameter, in analogy to P_r^*). In studies of the electrical conductance of polymers under different temperature and pressure conditions, Hartmann (105), using his own P-V-T equation (48) and building on the similiarity in form between the Doolittle relation for viscosity and Walden's Rule for conductance, found that an assumption of $P_c^*/P^* = 3.4$ was required (P_c^* indicates a reducing parameter for conductance). Browstow and Szymanski (106) have recently reviewed the variation in scaling pressures needed to describe various transport properties.

Given the latitude in scaling assumptions described in the literature and the over-estimation when $P_r^* = 2P^*$ is used in fitting the data of Cogswell and McGowan (10), it is not unreasonable to try other scaling assumptions for P_r^*.

An additional concern was the role of pressure in increasing the modulus. The value $P_r^* = 3.25P^*$ was chosen to calculate the shift factor for the time constant (equation(4-12)) and equation (5-3) was used to calculate the modulus shift factor. The results, in ratio form, are shown in Figure 5.10. The use of these parameters gives an improvement in the fit compared with Figure 5.9, although the agreement is not entirely satisfactory when the temperature is significantly different from the range 170-180°C. The influence of temperature at high pressures can undoubtedly be adjusted by changing

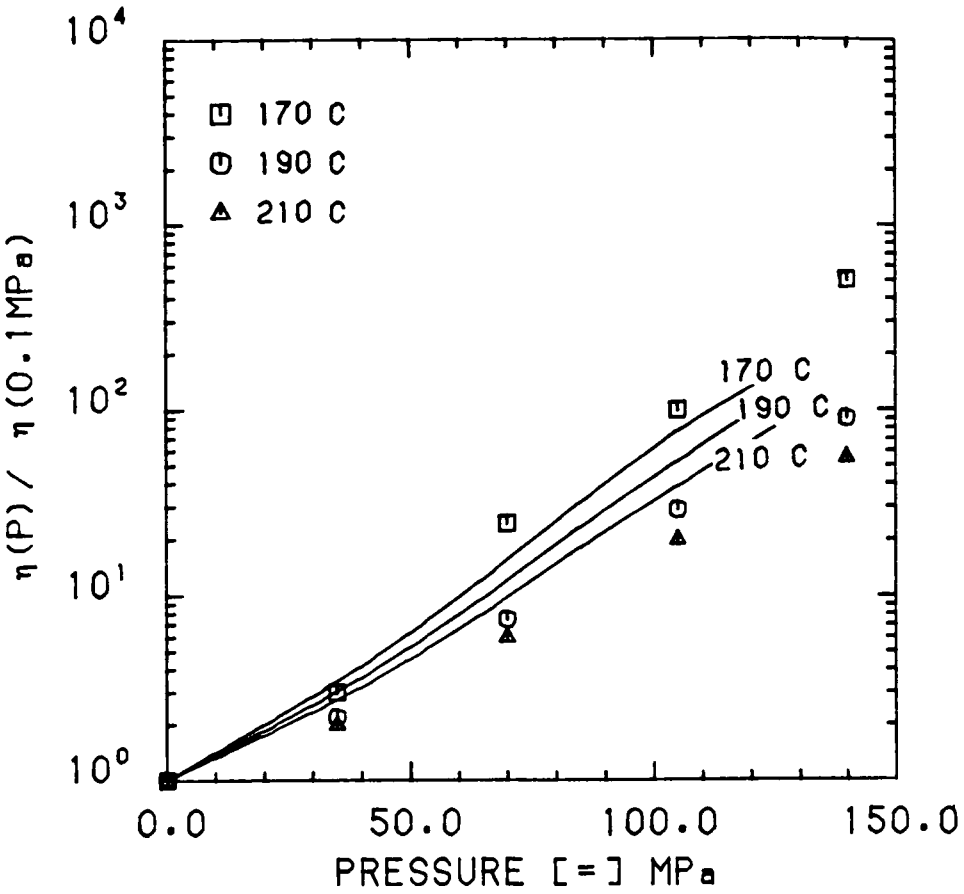

Figure 5.10 Ratio of zero shear viscosities vs. pressure, compared to pressure dependent shear modulus theory lines. Theory lines assume $P_r^* = 3.25P^*$ and that modulus is a function of pressure as in equation (5-2).

the "effective temperature", the temperature analog of introducing the empiricism or $P_r^*=2.0P^*$. A step in this direction is Figure 5.11 in which the effective temperature, $T_r^*=1.1T_r$, was used. This assumption required the adjustment of the P_r^* assumption to $P_r^*=4.0P^*$. A suitable fit can undoubtedly be made, but the use of such large scaling factors casts doubt in the validity of the P-V-T equation itself. Since the data of the present work are mostly at 180°C, this modification was not pursued further.

One feature of the curves in Figure 5.10 is of qualitative interest. The combination of making the modulus, as well as the time constant, a function of pressure introduces a small but pronounced non-linearity in the semi-log plot shown there; because of the dominant effect of the time constant at large pressures, one can expect the plot to become linear (like Figure 5.9) at higher pressures. A close inspection of the data shows that they also show a small "S-shaped" non-linearity of the type predicted by the theory, although the changes are so small that one would want independent verification before any definitive conclusion is reached.

Summary of the Model for Pressure Effects over All Shear Ranges

Figure 5.12 is a summary plot of the proposed model and the data over the entire range, extending from the low (but unknown) shear rates of Cogswell and McGowan (10) to the high shear rates of the present work. The theory lines are drawn from equation (4-16) using shift factors provided by the simplified fit of the Simha-Somcynsky theory (equation (4-12)), evaluated at 180°C and assuming $P_r^*=3.25\ P^*$. The modulus as a function of pressure is taken from equation (5-3) and

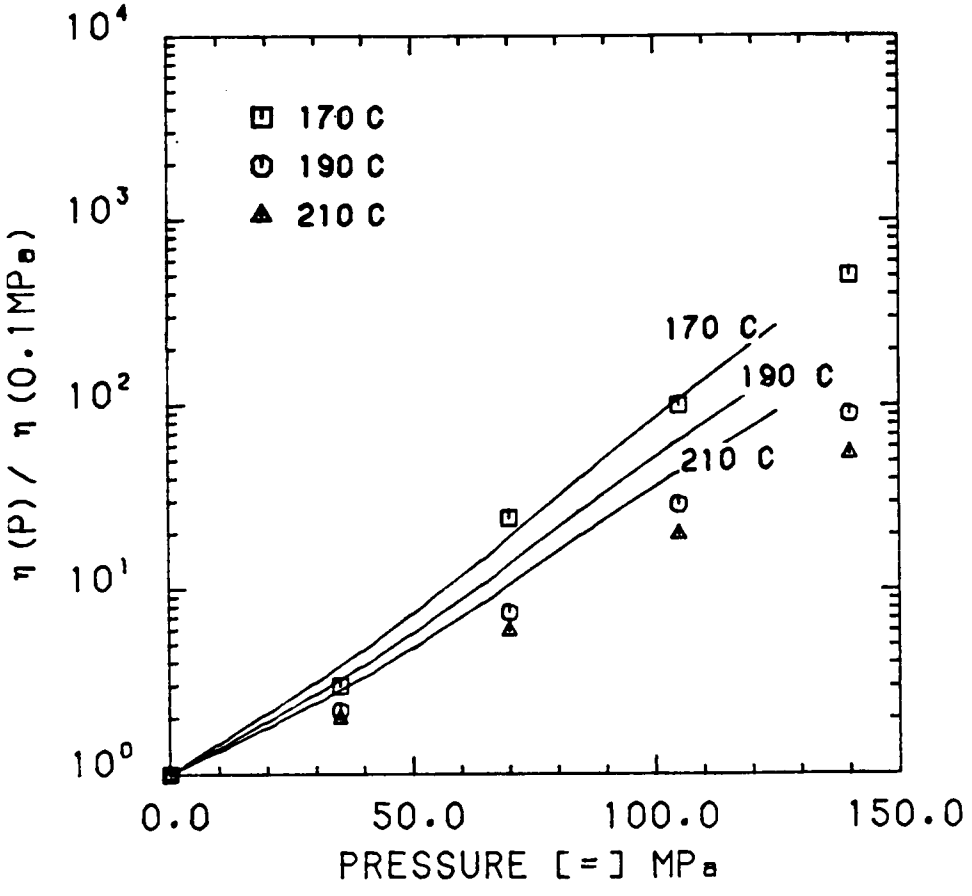

Figure 5.11 Ratio of zero shear viscosities vs. pressure, compared to pressure dependent shear modulus theory lines using an adjustable reducing temperature. Theory lines assume that modulus is a function of pressure as in equation (5-3), and additionally that $T_r^*=1.1T^*$ and $P_r^*=4.0P^*$.

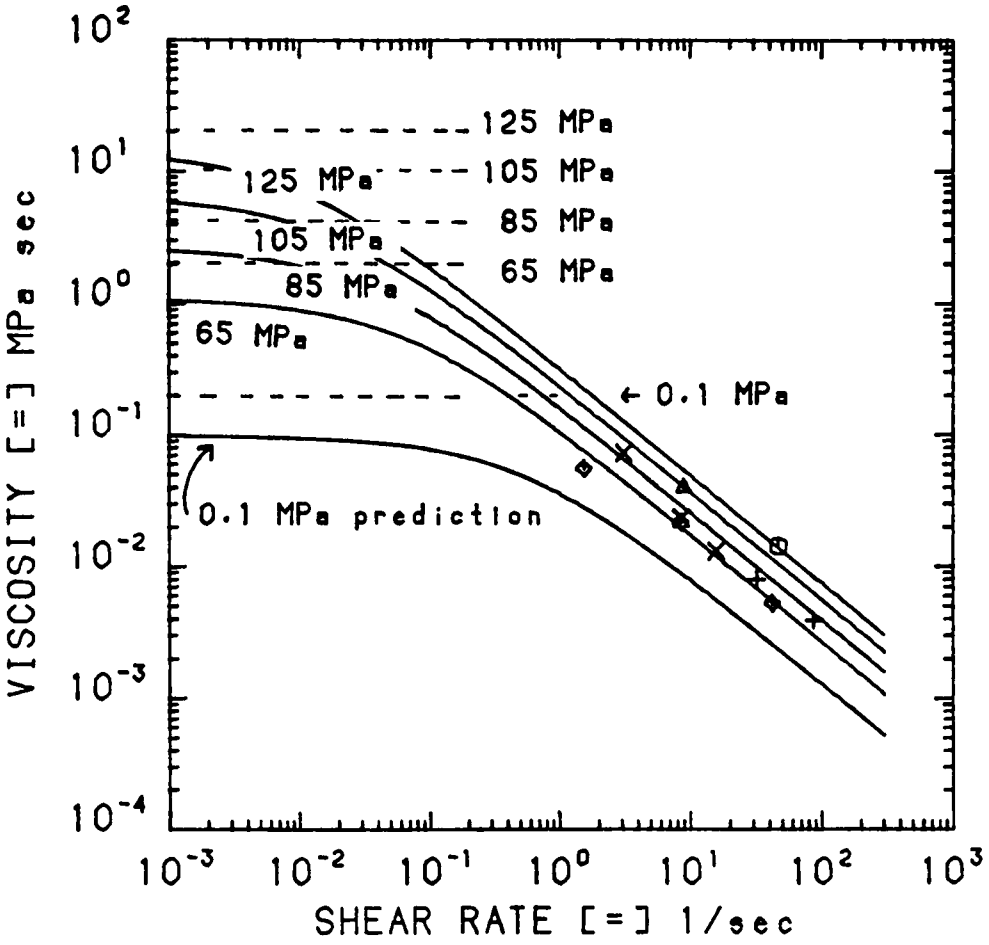

Figure 5.12 Summary of theoretical fits and data as a function of shear rate. The solid lines are the prediction from equation (5-3). The dashes indicate zero shear rate data of Cogswell and McGowan (10) interpolated for temperature (to 180°C) and pressures as shown; the dashed lines are in the probable shear rate range of their experiment.

the material constants τ_0, G_0, and "a" have the values noted in the previous section. The high pressure, high shear rate data from the present work are reproduced from Figure 5.5 (page 53). The high pressure, low shear rate data of Cogswell and McGowan (10) are represented as horizontal dashed lines, the vertical position showing the appropriate levels of viscosity and the horizontal length of the lines showing an estimated of the shear rate range in which it is believed the data were taken. Interpolated values were taken from their data in order that the temperature and the four pressures would correspond to those used in the present work.

Although data from medium shear rates are obviously lacking, the theory gives a suprisingly good fit for both high and low shear rates, although the fit in the latter case may be fortuitous. As noted in Chapter 4, one must typically use a spectrum of moduli and time constants, rather than one pair of constants, as in the present model, to obtain fits over wide ranges of shear rate. The choice of the pair τ_0 and G_0, and the accompanying non-linear parameter "a", were mostly dictated by the high shear rate data and thus a fit there is to be expected. Nonetheless, it is clear that the model does properly represent the essential features of the data and therefore provides a good starting point for more extensive correlations. Also the model provides a clear mathematical summary of the principal conclusion of the present work--namely, that viscosities vary more strongly with pressure at low shear rates than at high shear rates, the former regime being strongly influenced by the time constants and the latter, by the modulus.

CHAPTER 6

CONCLUSIONS

The present work was concerned mainly with the measurement and analysis of the viscosity of a polymer melt (polystyrene) at high shear rates and high pressures (up to 125 MPa). The data were analyzed, however, in a more general framework which includes low shear rate data from the literature. The main conclusions to be drawn from these studies are as follows:

1. Experimental results at high pressures and high shear rates show that the increase in viscosity with pressure is considerable (about six-fold at a pressure of 125 MPa), although not nearly so high as might be expected from zero shear data (over 100-fold at the same pressure). The present results at high shear rates are reasonable when compared to the limited amount of prior experimental data. Viscosity increases in the present work fall below those of Ito, made at typical processing shear rates ($\approx$1-100 sec^{-1}), and above those of Semjonow, made at a constant high shear rate (40 sec^{-1}).

2. At high pressures and high viscosities the possibility of time effects in the die flow must be considered. Time effects are almost surely present, as they probably are in all capillary experiments at high shear rates (short residence times), but they are neglected here. In temperature studies one typically uses a variety of die lengths and die diameters and concludes that such effects are negligible if there is data superposition. In the present work it was only possible to explore the effects of two dies (of different

diameter). Although these are limited results, superposition was achieved and consequently time effects in the die were neglected. That time effects can be neglected in any experiment at high shear rates is difficult to justify theoretically because of the high material time constant involved, compared to the residence time. An explanation for neglecting time effects in such flows may lie in the fact that materials at high shear rates tend to the condition of a "yielding solid" (that is, to a condition of constant stress). This limiting condition can be seen in the idealized model presented by equations (4-13) and (4-14) at the asymptote of high shear rates.

3. In practice the data obtained at high pressures (in the upstream and downstream chambers) also involved high pressure drops through the die. If one makes the usual assumption of adiabatic flow, these high pressure drops translate into high temperature rises, due to viscous heat generation. However a heat transfer analysis showed that heat transfer to the wall almost entirely compensated for the viscous heat generation. Thus essentially isothermal conditions could be assumed.

4. At low shear rates a free volume analysis coming from the Simha-Somcynsky (S-S) equation of state has previously been shown to be useful for analyzing both pressure and temperature effects. In the present work the predictions of the S-S theory, which is of a complex mathematical form, were fit with empirical but mathematically tractable functions. In the most useful form one can show that the fit reduces to the standard Williams-Landel-Ferry (WLF) equation for the temperature shift factor.

5. In such analyses one needs to note that the viscosity is a product of the modulus and a time constant. In the rubbery state one makes the customary assumption that the modulus is proportional to the absolute temperature, an almost negligible correction in the temperature range investigated. In the more general case, in which both time and pressure effects are being studied, one must deal with how the modulus varies with pressure as well. Results from the literature show the modulus increases with pressure, although there is considerable scatter in the data. In the present analysis, the effect of pressure on modulus was treated empirically, with the resulting correlation falling within the bounds of prior data.

6. The major experimental observation of the present work is that the effect of pressure is substantially diminished at high shear rates; that is, a large increase in pressure does not produce the large increases in viscosity that one sees at low shear rates. This is consistent with related findings that the effects of temperature and molecular weight also tend to be diminished at high shear rates. Using any shear rate-dependent rheological model, one can show that the effect of the time constant on viscosity is increasingly less important as the shear rate is increased, with the effect of modulus becomes more pronounced. In the present work this observation was quantified in terms of a particular rheological equation (the Bogue-White model). Coupling this model with the shift factor equations for the time constant and the modulus, the effects of pressure (and also temperature) on viscosity can be correlated over a wide spectrum of shear rates.

REFERENCES

REFERENCES

1. P. W. Bridgman, "The Physics of High Pressure," Macmillan, New York, 1931.

2. B. Maxwell and A. Jung, Modern Plastics, 57, No.1, 174 (1957).

3. R. F. Westover, SPE Trans., 1, 14 (1961).

4. J. F. Carley, "SPE 17th ANTEC Technical Papers," Paper No. 25-4, (Jan. 1960).

5. K. Ito, M. Tsutsui, M. Dasajima, and T. Ojima, Applied Polymer Symposium No. 20, 109 (1973).

6. S. Y. Choi, J. Polym. Sci., A-2, 6, 2043 (1968).

7. R.C. Penwell and R.S. Porter, J. Polym. Sci., A-2, 9, 463 (1971).

8. R.C. Penwell, R.S. Porter and S. Middleman, J. Polym. Sci., A-2, 9, 731 (1971).

9. P. H. Goldblatt and R. S. Porter, J. Appl. Polym. Sci., 20, 1199 (1976).

10. F. N. Coswell and J. C. McGowan, Br. Polym. Jr., 4, 183 (1972).

11. F. N. Cogswell, Plastics and Polymers, 41, 39 (1973).

12. W. W. Graessley, S. D. Glasscock, and R. L. Crawley, Trans. Soc. Rheol., 14, 519 (1970).

13. K. Hellwege, W. Knappe, F. Paul and V. Semjonow, Rheol. Acta., 6, 165 (1967).

14. V. Semjonow, Rheol. Acta., 2, 138 (1962).

15. V. F. Ramsteiner, Rheol. Acta., 9, 374 (1970).

16. J. M. O'Reilly, "Effect of Pressure on Amorphous Polymers," in "Modern Aspects of the Vitreous State," J. D. Mackenzie, ed., vol. 3, Butterworths, Washington, 1964.

17. I. Havlicek, M. Ilavsky, and J. Hrouz, J. Macromol. Sci.- Phys., B21, 425 (1982).

18. H. Oels and G. Rehage, Macromolecules, 10, 1036 (1977).

19. J. M. O'Reilly, J. Polym. Sci., 57, 429 (1962).

20. K. Hellwege, W. Knappe, and P. Lehmann, Kolloid-Z, 183, 110 (1963).

21. G. Gee, Polymer, 7, 177 (1966).

22. A. Quach and R. Simha, J. Appl. Phys., 42, 4592 (1971).

23. P. Zoller, J. Polym. Sci.- Phys. Ed., 20, 1453 (1982).

24. G. Williams, Trans. Faraday Soc., 60, 1548 , 1556 (1964).

25. G. Williams, Trans. Faraday Soc., 61, 1564 (1965).

26. E. N. Dalal and P. J. Phillips, Macromolecules, 16, 890 (1983).

27. R. B. Bird, R. C. Armstrong, and O. Hassanger, "Dynamics of Polymer Liquids, Vol. I: Fluid Mechanics," Wiley, New York, 1977.

28. C. D. Han, K. U. Kim, N. Siskovic, and C. R. Huang, Rheol. Acta., 14, 533 (1975).

29. K. Osaki, N. Bessho, T. Kojimoto, and M. Kurata, J. Rheol., 24, 125 (1980).

30. A. S. Lodge, "Elastic Liquids," Academic Press, New York, 1964.

31. M. L. Williams, R. F. Landel, and J. D. Ferry, J. Amer. Chem. Soc., 77, 3701 (1955).

32. J. D. Ferry and R. A. Stratton, Kolloid-Z, 171, 107 (1960).

33. R. W. Fillers and N. V. Tschoegl, Trans. Soc. Rheol., 21, 51 (1977).

34. F. Bueche, J. Chem. Phys., 36, 2940 (1962).

35. A. Zosel, Kolloid-Z, 199, 113 (1964).

36. W. K. Moonan and N. W. Tschoegl, Macromolecules, 16, 55 (1983).

37. W. K. Moonan and N. W. Tschoegl, Int. J. Polym. Mater., 10, 199 (1984).

38. W. K. Moonan and N. W. Tschoegl, J. Polym. Sci.- Phys Ed., 23, 623(1985).

39. J. D. Ferry, "Viscoelastic Properties of Polymers," 3rd ed., p. 291, John Wiley and Sons, New York, 1980.

40. R. S. Spencer and G. D. Gilmore, J. Appl. Phys., 20, 502 (1949).

41. R. S. Spencer and G. D. Gilmore, J. Appl. Phys., 21, 523 (1950).

42. J. F. Carley, "Rheology," in "Introduction to Polymer Science and Technology," H. S. Kaufman and J. J. Falcetta, eds., p. 445, Wiley-Interscience, New York, 1977.

43. P. G. Tait, "Physics and Chemistry of the Voyage of H. M. S. Challenger," Vol. II, part IV, in "Scientific Papers," LXI (1888), Vol. II, p. 1, University Press, Cambridge, 1900.

44. L. A. Wood, Polym. Letters, 2, 703 (1964).

45. V. S. Nanda and R. Simha, J. Chem. Phys., 41, 3870 (1964).

46. O. Olabisi and R. Simha, J. Appl. Polym. Sci., 21, 149 (1977).

47. P. Zoller and H. H. Hoehn, J. Polym. Sci.-Phys. Ed., 20, 1385 (1982).

48. B. Hartmann and M.A. Haque, J. Appl. Polym. Sci., 30, 1553 (1985).

49. B. Cho, Polym. Eng. Sci., 25, 1139 (1985).

50. V. S. Nanda and R. Simha, J. Phys. Chem., 68, 3158 (1964).

51. V. S. Nanda, R. Simha, and T. Somcynsky, J. Polym. Sci. - Part C, 12, 277 (1966).

52. R. Simha and T. Somcynsky, Macromolecules, 2, 342 (1969).

53. R. Simha, Macromolecules, 10, 1025 (1977).

54. J. E. Lennard-Jones and A. F. Devonshire, Proc. Roy. Soc. Ser. A., 163, 53 (1937).

55. I. Prigogine, N. Trappeniers, and V. Mathot, Discussions Faraday Soc., 15, 93 (1953); also I. Prigogine, "The Molecular Theory of Solutions," North-Holland, Amsterdam, 1957;

56. R. Simha, Polym. Eng. Sci., 22, 74 (1982).

57. R. Simha, J. Rheol., 30, 639 (1986).

58. L. A. Utracki, Polym. Eng. Sci., 25, 655 (1985).

59. J. E. McKinney and R. Simha, Macromolecules, 7, 894 (1974).

60. P. Zoller, J. Polym. Sci. - Phys. Ed., 16, 1261 (1978).

61. R. K. Jain, R. Simha, and P. Zoller, J. Polym. Sci.-Phys. Ed., 20, 1399 (1982).

62. L. A. Utracki, Poly. Eng. Sci., 23, 446 (1983).

63. L. A. Utracki, Canad. J. Chem. Eng., 61, 753 (1983).

64. R. M. Shay, Jr. and J. M. Caruthers, J. Rheol., 30, 781 (1986).

65. J. G. Curro, R. R. Lagasse, and R. Simha, J. Appl. Phys., 52, 5892 (1981).

66. R. R. Lagasse and J. G. Curro, Macromolecules, 15, 1559 (1982).

67. B. Hartmann and M. A. Haque, J. Appl. Phys., 58, 2831 (1985).

68. T. S. Chow, Macromolecules, 17, 2336 (1984).

69. T. S. Chow, Polym. Eng. Sci., 24, 1079 (1984).

70. T. S. Chow, J. Rheol., 30, 729 (1986).

71. M. Litt, J. Rheol., 30, 853 (1986).

72. T. Takaki, M. S. Thesis in Chemical Engineering, The University of Tennessee, Knoxville (1973).

73. R. Racin, M. S. Thesis in Polymer Engineering, The University of Tennessee, Knoxville (1978).

74. T. Takaki and D. C. Bogue, J. Appl. Polym. Sci., 19, 419 (1975).

75. M. Matsui and D. C. Bogue, Trans. Soc. Rheol., 21, 133 (1977).

76. T. Matsumoto and D. C. Bogue, Trans. Soc. Rheol., 21, 453 (1977).

77. T. Matsumoto and D. C. Bogue, Polym. Eng. Sci., 18, 546 (1977).

78. R. Racin and D. C. Bogue, J. Rheol., 23, 263 (1979).

79. C. J. Wust and D. C. Bogue, J. Appl. Polym. Sci., 28, 1931 (1983).

80. B.D. Snow, P. Potnis, and D.C. Bogue, J. Rheol., 28, 517 (1984).

81. F.N. Cogswell, "Polymer Melt Rheology," Godwin, London, 1981.

82. H. Leaderman, Text. Res., 11, 171 (1941).

83. F. Shwarzl and A. J. Staverman, J. Appl. Phys., 23, 838 (1952).

84. H. Markovitz, J. Polym. Sci.: Polymer Symp. No. 50, 431 (1975).

85. A. V. Tobolsky and R. D. Andrews, J. Chem. Phys., 13, 3 (1945).

86. L. R. G. Treloar, "The Physics of Rubber Elasticity," 2nd. Ed., Oxford University Press, London, 1958.

87. A. K. Doolittle and D. B. Doolittle, J. Appl. Phys., 28, 901 (1957).

88. Dr. Leszek Utracki, private communication.

89. D. A. Carey, C. J. Wust, Jr., and D. C. Bogue, J. Appl. Polym. Sci., 25, 575 (1980).

90. D. C. Bogue and J. L. White, "Engineering Analysis of Non-Newtonian Fluids," NATO Agardograph 144, 1970.

91. S. Nam and D. C. Bogue, Ind. Eng. Chem. Fundam., 23, 1 (1984).

92. W. Deitz and D. C. Bogue, Rheol. Acta., 17, 595 (1978).

93. T. Masuda, M. Takahashi, and S. Onogi, Applied Polymer Symposium No. 20, 49 (1973), and T. Masuda, Ph.D. Dissertation in Polymer Chemistry, Kyoto University, Kyoto (1973). See also, E. Kamei and S. Onogi, Polym. J., 8, 347 (1976).

94. W. W. Graessley, J. Chem. Phys., 43, 2696 (1965).

95. Z. Tadmor and C. G. Gogos, "Principles of Polymer Processing," Wiley-Interscience, New York, 1979.

96. H. L. Toor, AIChE J., 3, 92 (1957).

97. D. C. Bogue, private communication.

98. R. B. Bird, W. E. Stewart, and E. N. Lightfoot, "Transport Phenomena," Wiley, New York, 1960.

99. W. H. McAdams, "Heat Transmission," McGraw Hill, New York, 1954.

100. J. Brandup and E. H. Immergut, eds., "Polymer Handbook," Wiley-Interscience, New York, 1966.

101. T. G. Fox and P. J. Flory, J. Appl. Phys., 21, 581 (1950).

102. T. G. Fox and P. J. Flory, J. Amer. Chem. Soc., 70, 2384 (1948).

103. R. F. Boyer, J. Polym. Sci.-Part C, 14, 267 (1966).

104. L. A. Utracki, J. Macromol. Sci., B10, 477 (1974).

105. B. Hartmann, J. Rheol., 30, 843 (1986).

106. W. Browstow and W. Szymanski, J. Rheol., 30, 877 (1986).

107. D. C. Bogue, Ind. Chem. Eng. Fundam., 5, 253 (1966).

108. R. B. Bogue, West Georgia College, Carrollton, GA, private communication.

APPENDICES

APPENDIX A

FORTRAN PROGRAMS TO SOLVE SIMHA-SOMCYNSKY

EQUATION OF STATE SIMULTANEOUSLY

```
c...Program for VOLUME-TEMPERATURE plots
c
c...forssvt.for
c
c
c  Method: Two Simha-Utracki equations are solved for T, then
c          T is eliminated.  The resulting equation is solved
c          for P.  A low temperature phi is chosen as a constant
c          and y is varied until P converges for that isobar.
c          This brute force method produces some T (and a V)
c          for each phi.  Phi is then incremented for the next
c          (higher) T.  Correct phi ranges for each isobar are
c          obtained by trial and error, although high temperature
c          starting phi's can be estimated from Utracki's output.
c          Initial y's don't seem to matter.
c
c
c Good for vt  t going up  w/phi decreasing 11:26 july 4 1986
c
c
c...program ssvt.for
c
c
c...program to produce isobars of v-t data from simha's
c...equations of state
c
c
        dimension ppr(10), yy(10), pp(10), pphi(10)
c...input number of temps file
        open ( unit = 30, status = 'old', file= 'ssvtin.in')
        read ( 30, *) nn
        do 3 I = 1, nn
c...pressure, temperature, volume are designated pr,tr,and vr
c...because they are generic reduced parameters
c...initial value for phi, p is Utracki's phi=(vy)**-1
        read ( 30, *) ppr(i), yy(i), pp(i), pphi(i)
3       continue
        close ( unit =30, status = 'save')

c...Output files
        open (unit = 31, status= 'old', file ='ssvtout.out')
        open ( unit = 32, status = 'old', file = 'ssvt.dat')
        open ( unit = 33, status = 'old', file = 'ssvtlprout.out')
```

```
        ii = 1

c...constant constants
        q = 1.0 / 3.0
        r = .8908987

        do 4 iii = 1, nn
         p =  pp(ii)
         pr = ppr(ii)
         y  = yy(ii)

c...write data statement in pressure-volume output file
        write ( 32, 99)
99      format ( 1x, 'DATA')

c...Write columns heads in output file
        write (31,100)
100     format (//,2x,'n',3x,'tr',5x,'vr',5x,'pr',7x,'y',7x,'phi',
     1          6x,'y*vr')
        write (33,105)
105     format (//,2x,'n',3x,'tr',5x,'vr',5x,'pr',7x,'y',7x,'phi',
     1          6x,'y*vr',4x,'ps',4x,'tk',6x,'tc',7x,'v(cc/g)',
     2           3x,'v(m3/kg)',3x,'p(mpa)')


C...n counts for non-converging sequence kick out
5       n=0


c...variable constants
1       a=1.0 +(1.0/y)* log(1.0-y)
        b= 2.409 - 3.033 * p**2.0
        c = -q + (r * y * p**(q))
        g = 1.0 / (1.0 - r * y * (p**(q)) )
        vr = (p*y)**(-1.0)
        f=p**2.0*(1.011*p**2.0-1.2045)


c...actual 2nd Simha-Utracki equation
        z = (b*y*p**2.0)/(6.0*(a-c*g))

c...combined utracki-simha equations, t elimnated
        prnext = g*z/vr + 2*y*f/vr

        n=n+1
        if (n .ge. 50) goto 10
        if (abs(prnext-pr) .gt. .0000001) then
                e = pr - prnext
                d= 2.0
c...for this simple case 4.0 converges in 5 loops
                ynext=y - d * e
                y=ynext
```

```
                goto 1
        endif

10      tr = z
        vry = 1.0 / p
        write (31, 13) n, tr, vr, pr, y, p, vry
13      format (/,1x,i2,x,f8.6,x,f6.4,x, f7.5,x,f7.5,x,f6.4,x,f7.6)
        write (33, 12) n, tr, vr, pr, y, p, vry, tr*12680.0,
     1                  tr*12680.0-273.15, vr*.960, vr*.00096,
     2                  pr*745.0
12      format (/,1x,i2,x,f8.6,x,f6.4,x, f7.5,x,f7.5,x,f6.4,x,f7.6
     1           ,10x,f7.3,x,f7.3,x,f8.6,x,f8.6,x,f6.2)
        write ( 32, 14) tr*12680, vr*.960
14      format ( 1x, f7.3, 2x, f7.5)
        p = p - .00001
        if ( p .lt. pphi(ii)) goto 15
        goto 5
15      II = ii + 1
4       continue
        close (unit = 31, status = 'save')
        close (unit = 32 , status = 'save')
        close (unit = 33 , status='save')
        stop
        end
```

```
c...Program for VOLUME-PRESSURE plots
c
c...forssvp.for
c
c  Method:With the second S-S/Utracki equation solve for T.
c         Pick a certain phi and try different y's until T
c         converges (a brute force method used).  Put these
c         values in the first S-S equation and solve for P.
c
c
c...program to produce isotherms of v-p data from simha's
c...equations of state
c
c
        dimension ttr(10), yy(10), pp(10), pphi(10)
c...input number of temps file
        open ( unit = 30, status = 'old', file= 'ssvpin.in')
        read ( 30, *) nn
        do 3 I = 1, nn
c...pressure, temperature, volume are designated pr,tr,and vr
c...because they are generic reduced parameters
c...initial value for phi, p is Utracki's phi=(vy)**-1
        read ( 30, *) ttr(i), yy(i), pp(i), pphi(i)
3       continue
        close ( unit =30, status = 'save')

c...Output files
        open (unit = 31, status= 'old', file ='ssvpout.out')
        open ( unit = 32, status = 'old', file = 'ssvp.dat')
        open ( unit = 33, status = 'old', file = 'ssvplprout.out')

        ii = 1

c...constant constants
        q = 1.0 / 3.0
        r = .8908987

        do 4 iii = 1, nn
         p =  pp(ii)
         tr = ttr(ii)
         y  = yy(ii)

c...write data statement in pressure-volume output file
        write ( 32, 99)
99      format ( 1x, 'DATA')

c...Write columns heads in output file
        write (31,100)
100     format (//,2x,'n',3x,'tr',5x,'vr',5x,'pr',7x,'y',7x,'phi',
     1          6x,'y*vr')
        write (33,105)
105     format (//,2x,'n',3x,'tr',5x,'vr',5x,'pr',7x,'y',7x,'phi',
```

```
     1          6x,'y*vr',4x,'ps',4x,'tk',6x,'tc',7x,'v(cc/g)',
     2           3x,'v(m3/kg)',3x,'p(mpa)')


C...n counts for non-converging sequence kick out
5       n=0


c...variable constants
1       a=1.0 +(1.0/y)* log(1.0-y)
        b= 2.409 - 3.033 * p**2.0
        c = -q + (r * y * p**(q))
        g = 1.0 / (1.0 - r * y * (p**(q)) )
        vr = (p*y)**(-1.0)
        f = p**2.0*(1.011*p**2.0-1.2045)

c...actual 2nd Simha-Utracki equation
10      trnext = (b*y*p**2.0)/(6.0*(a-c*g))

        n=n+1
        if (n .ge. 50) goto 10
        if (abs ( trnext - tr) .gt. .0000001) then
                e = tr - trnext
                d= 2.0
c...often converges in 5 loops
                ynext=y - d * e
                y=ynext
                goto 1
        endif

c...actual 1st simha equation
        pr = tr/vr*(g+2.0*y*f/tr)

        vry = 1.0 / p
        write (31, 13) n, tr, vr, pr, y, p, vry
13      format (/,1x,i2,x,f8.6,x,f6.4,x, f7.5,x,f7.5,x,f6.4,x,f7.6)
        write (33, 12) n, tr, vr, pr, y, p, vry, tr*12680.0,
     1                  tr*12680.0-273.15, vr*.960, vr*.00096,
     2                  pr*745.0
12      format (/,1x,i2,x,f8.6,x,f6.4,x, f7.5,x,f7.5,x,f6.4,x,f7.6
     1           ,10x,f7.3,x,f7.3,x,f8.6,x,f8.6,x,f6.2)
        write ( 32, 14) pr*745.0, vr*.960
14      format ( 1x, f7.3, 2x, f7.5)
        p = p + .001
        if ( p .gt. pphi(ii)) goto 15
        goto 5
15      II = ii + 1
4       continue
        close (unit = 31, status = 'save')
        close (unit = 32 , status = 'save')
        close (unit = 33 , status='save')
        stop
```

APPENDIX B

Pressure Drop - Flow Rate Relationship For Non-Newtonian Flow in a Tube

The relationship between pressure drop and flow rate for developed flow in a tube has been worked out for several of the well-known rheological models (see, for example, Bird et. al. (98)). In the analysis below this relationship is developed for the so-called Bogue-White model, which was proposed by Bogue (107) in 1966 and later modified in terms of a different strain tensor by Bogue and White (91). In shear flow in a tube this model takes the form

$$\sigma_{rz} = \frac{G\tau(dv_z/dr)}{1 + a\tau\,|dv_z/dr|} \qquad \text{(A-1)}$$

where σ_{rz} is the shear stress, dv_z/dr is the velocity gradient, G is an elastic modulus, τ is a time constant, and 'a' is an adjustable (empirical) parameter. In the analysis here, we consider only the single element case (one G and one τ).

The analysis starts with the force balance on a radial element dr (98):

$$0 = -p' + \frac{1}{r}\frac{d(r\sigma_{rz})}{dr} \qquad \text{(A-2)}$$

where $p' = \Delta p / \Delta x$, p is the pressure at some position x, and r is the radius. Since $\sigma_{rz} = 0$ at $r = 0$, this equation can be solved to give

$$\sigma_{rz} = p'\,(r/2) \qquad \text{(A-3)}$$

Introducing equation (A-1) and noting that dv_z/dr is negative, one obtains

$$\frac{G\tau(dv_z/dr)}{1 + a\tau\,|dv_z/dr|} = p' \frac{r}{2} \qquad \text{(A-4)}$$

This equation can be integrated but leads to an awkward result that does not reduce easily to the Newtonian case. It is more convenient to expand the r-dependent integrand in a series as follows (D. C. Bogue (97)):

$$dv_z = -r\,dr \left[\frac{1}{\beta - \alpha r}\right] = \frac{-r\,dr}{\beta}\left[1 + \frac{\alpha}{\beta} r + \frac{\alpha^2}{\beta^2} r^2 + \ldots\right] \qquad \text{(A-5)}$$

where $\alpha = a\tau$, and $\beta = -2G\tau/p'$. This integrates to the result

$$v_z = \frac{-r^2}{2\beta} - \frac{\alpha\, r^3}{\beta^2\, 3} - \frac{\alpha^2\, r^4}{\beta^3\, 4} - \ldots + C \qquad \text{(A-6)}$$

Introducing the boundary condition that $v_z = 0$ at $r = R$ leads to

$$C = \frac{R^2}{2\beta} - \frac{\alpha\, R^3}{\beta^3\, 3} - \frac{\alpha^2\, R^4}{\beta^3\, 4} + \ldots \qquad \text{(A-7)}$$

To obtain the volumetric flow rate Q, one forms the integral

$$Q = \int_0^R v_z(r)\, 2\pi r\, dr \qquad \text{(A-8)}$$

which leads finally to the result

$$Q = \frac{\pi R^4 (-p')}{8G\tau} \left[1 + \frac{4}{5}\chi + \frac{2}{3}\chi^2 + \frac{4}{7}\chi^3 + \ldots \right] \qquad \text{(A-9)}$$

where $\chi = -(Rap')/(2G)$.

The series does not converge for $\chi \geq 1$ and converges only slowly as χ nears unity. Fortunately, however, R.B. Bogue (108) observed that the series in the bracket can be stated in closed form, giving the result

$$Q = \frac{\pi R^4 (-p')}{8G\tau} \left[1 + \frac{4}{\chi^4} \left[-\ln(1-\chi) + \chi + \frac{\chi^2}{2} + \frac{\chi^3}{3} + \frac{\chi^4}{4} \right] \right] \qquad \text{(A-10)}$$

It is obvious that the series solution (equation (A-9)) reduces to the Newtonian case (the Hagen-Poseuille equation) as χ approaches zero:

$$Q = \frac{\pi R^4 (-p')}{8G\tau} \qquad \text{(A-11)}$$

It is not at all evident that the closed solution (equation (A-10)) reduces properly in this limit. By applying L'Hospital's rule four times, however, R.B. Bogue (108) was able to show that the closed solution does, in fact, reduce to equation (A-11) as χ approaches zero. Equation (A-10) is, then, a completely general solution for the rheological model stated in equation (A-1).

APPENDIX C

180°C High Pressure Viscosity Data

Upper die dimensions: D=.071", L/D=20

p_{ave}[=]MPa	Δp[=]MPa	$\dot{\gamma}_w$[=]sec^{-1}	$\eta_{w,corrected}$[=]MPa sec
124.0	89.2	46.6	0.0143
106.8	45.1	8.94	0.0402
82.7	48.8	87.0	0.0039
75.8	23.4	8.58	0.02325
69.0	21.4	8.48	0.02162
58.0	27.9	41.9	0.00525
50.3	12.7	4.11	0.02353
44.8	16.5	16.38	0.0072
44.1	15.8	8.11	0.01595
41.3	13.8	8.06	0.013766
40.0	11.0	4.03	0.0207
38.6	16.2	16.2	0.00718
37.2	11.4	4.0	0.02148
31.7	11.3	7.96	0.01143
30.3	4.4	1.6	0.02194
27.6	8.4	4.0	0.0161
24.8	8.3	4.0	0.0158
24.8	5.1	1.6	0.0251
22.4	5.0	1.6	0.0246
19.6	2.0	0.79	0.0207
18.6	4.1	1.56	0.02025
17.4	3.9	0.78	0.0401
17.2	2.8	0.78	0.0284
12.6	1.7	0.77	0.0178

Upper die dimensions: D=.071", L/D=20

p_{ave}[=]MPa	Δp[=]MPa	$\dot{\gamma}_w$[=]sec^{-1}	$\eta_{w,corrected}$[=]MPa sec
84.4	31.0	32.06	0.008
74.4	24.7	15.74	0.0131
73.0	28.8	3.13	0.0726
60.3	13.7	1.55	0.0555
53.5	24.7	7.63	0.027
52.0	14.5	3.03	0.0399
51.7	13.6	1.52	0.0758
36.3	6.5	0.74	0.0806
34.4	6.1	0.74	0.0755
34.4	6.5	0.74	0.0801
34.4	6.1	1.48	0.0285
34.0	10.1	2.96	0.0185
33.3	8.8	1.48	0.0487
32.0	9.0	1.48	0.0496
31.3	7.4	1.48	0.0409

VITA

Paul D. Driscoll was born in Redwood Falls, Minnesota on January 10, 1960. He graduated from Redwood Falls High School in 1978. He attended Northwestern University, graduating with a B.S. in Materials Science and Engineering in 1982.

After working for two years at Desoto, Inc. in Des Plaines, Illinois, he enrolled in the Polymer Engineering program at The University of Tennessee. In December, 1986, a M.S. degree in Materials Science and Engineering was obtained. After completion of studies at The University of Tennessee, the author left for Japan to begin a 1 1/2 year Monbusho research scholarship at Kyoto University in the Department of Polymer Chemistry of the School of Engineering.